Multi-parameter topographical analysis of the subchondral bone in healthy and osteoarthritic human patellae

Inauguraldissertation

zur

Erlangung der Würde eines Dr. sc. med.

vorgelegt der

Medizinischen Fakultät

der Universität Basel

von

Sebastian Höchel

aus Matgendorf, Deutschland

Basel, 2018

Genehmigt von der Medizinischen Fakultät
auf Antrag von

Professor Dr. med. Markus Gerber, Basel (President of PhD committee)
Professor Dr. med. Magdalena Müller-Gerbl, Basel (Thesis supervisor)
Professor Dr. phil. Bert Müller, Allschwil (Co-supervisor)
Professor Dr. med. Dr. h.c. Reinhard Putz, München (External expert)

Basel, den 26.02.2018

Prof. Dr. med. Thomas Gasser
Dekan, Universität Basel

Table of content

“It seems almost doubtless that the bony trabeculae disappear where, as a result of a curvature, they are no longer stressed. New bony elements must develop where the material is stressed as a result of bony regeneration or of curvature of the bone.
… This leads us to the important conclusion that, in the proximal end of the human femur, bone is present only along the mathematical stress trajectories. Bone thus is built along the compression and tension lines.“

(*Julius Wolff,* 1877 [1])

1 Introduction

1.1 The principles of “morphology reveals biomechanics”

“To understand the law of bone remodeling requires precise knowledge of the internal architecture of normal bone…” (*Julius Wolff* [2])

Following this preliminary words in his 1892 published treatise of the architecture of bone, Julius Wolff aimed to describe a general concept of bone´s functional adaptation to mechanical loading and explain it by mathematical theories. Ever since, these theories, often loosely referred to as “Wolff´s law”, became cornerstones in the concept of functional adaptation. They marked the beginning of the understanding of the relation between biomechanical demands and morphological expression and became focal points of research for more than a century.

This era of research following “Wolff´s law” culminated in 1960 with the investigations of Friedrich Pauwels, who described the interchange between form and function within the human body not only for bone, but for other components of the locomotor apparatus as well. His defined theory of the “causal histogenesis” describes bone as well as soft tissue structures to be optimally adapted to the long-term load distribution in a defined area [3]. Following these accomplishments, Tillmann et al. [4] described the increase and decrease of tissue in 1971 as response to the range of stress and Carter et al. [5] established the definition of the “loading history of bone” in 1989.

The basic concept of the stated theories by Julius Wolff were explained and underlined by the example of the proximal end of the human femur. In his opinion, this was the most appropriate part of the body to illustrate his concepts. From the architecture of the femoral head and neck, direct relations to mathematical terms can be drawn and some work on the description of the internal morphology was already done.

More precisely, Wolff quotes the work of the English author F. O. Ward, who firstly published a schematic picture of the internal architecture of the femoral head and neck in 1838. In the published book of osteology, Ward presents a coronal section and compares the trabecular arrangement to a crane (lamp bracket). In Wards interpretation, the trabecular arrangement following compressive and tensile stresses developed by the loading of the bone and can be clearly differentiated.

The distinguished three groups of trabeculae form (a) an archway that corresponds to the column of the crane; (b) a set of tensile stressed fibers representing the cross piece; as well as (c) a compressive group which resembles the general support of the crane (Fig. 1) [6].

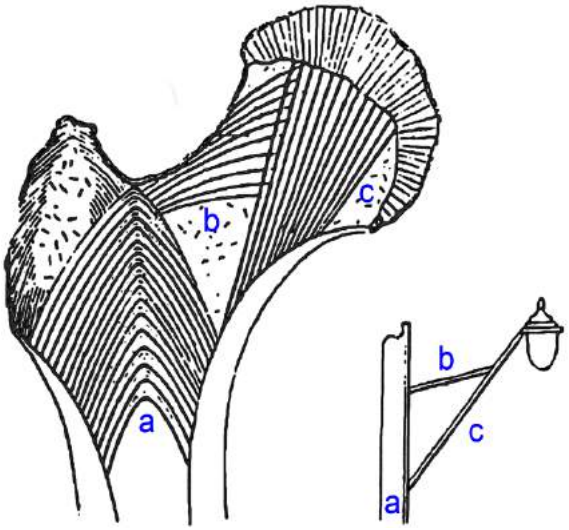

Figure 1 *Ward´s distinguished groups of trabeculae in a coronal section through the center of the proximal end of the femur (1838) and the compared lamp bracket.*

Julius Wolff used these descriptions as base and investigated the pattern of the trabeculae further. He aimed to understand more about the three dimensional arrangements and analyzed sections in all three different planes and finds an even more complicated structural situation. He defines 50 trabeculae originating from the medial and 50 from the lateral side which run towards their opposite cortical wall of the head and neck of the human femur. In doing so, they intersect at 90° angles and insert perpendicular to the inner surface of the cortical bone (Fig. 2).

To explain his findings of bone formation in a mathematical manner, he discussed the results with his colleague Karl Culmann from Zürich. Culmann, one of the leading engineers at that time, was head of the department for engineering science at ETH. Together, they discovered that the lines of compression and tension within the trabecular architecture of the femoral head are equally arranged to the ones in the newly designed Fairbairn crane that was built all over Europe since the 1850´ (Fig. 2). They then realized, that due to the incoming load of the human pelvic bone, the femur, as well as the crane, is stressed in bending. Consequently, the trabeculae originating from the medial side are under compression, the ones from the lateral side are under tension. If there were a lack of trabeculae or an insufficiency, the bone would collapse.

The mathematics performed by Culmann assumed a uniformly distributed load of about 30 kg at the area around point (a) (Fig. 2). This would account roughly to the inactive standing phase of an adult human. The approximated compressions at the marked intersection points range from (b) 5.7 kg, (c) 51.6 kg, to the maximum of 163.3 kg (d) (Fig. 2). Given these results, one can understand why the cortical bone, which is composed of dense trabecular, is relatively thin in areas just beneath the articular cartilage and increasing in size and volume towards the shaft. In distant regions of the center of the applied load, the cancellous trabeculae converge to form a thick cortical bone which in its extension towards the diaphysis has to bear the greatest loads.

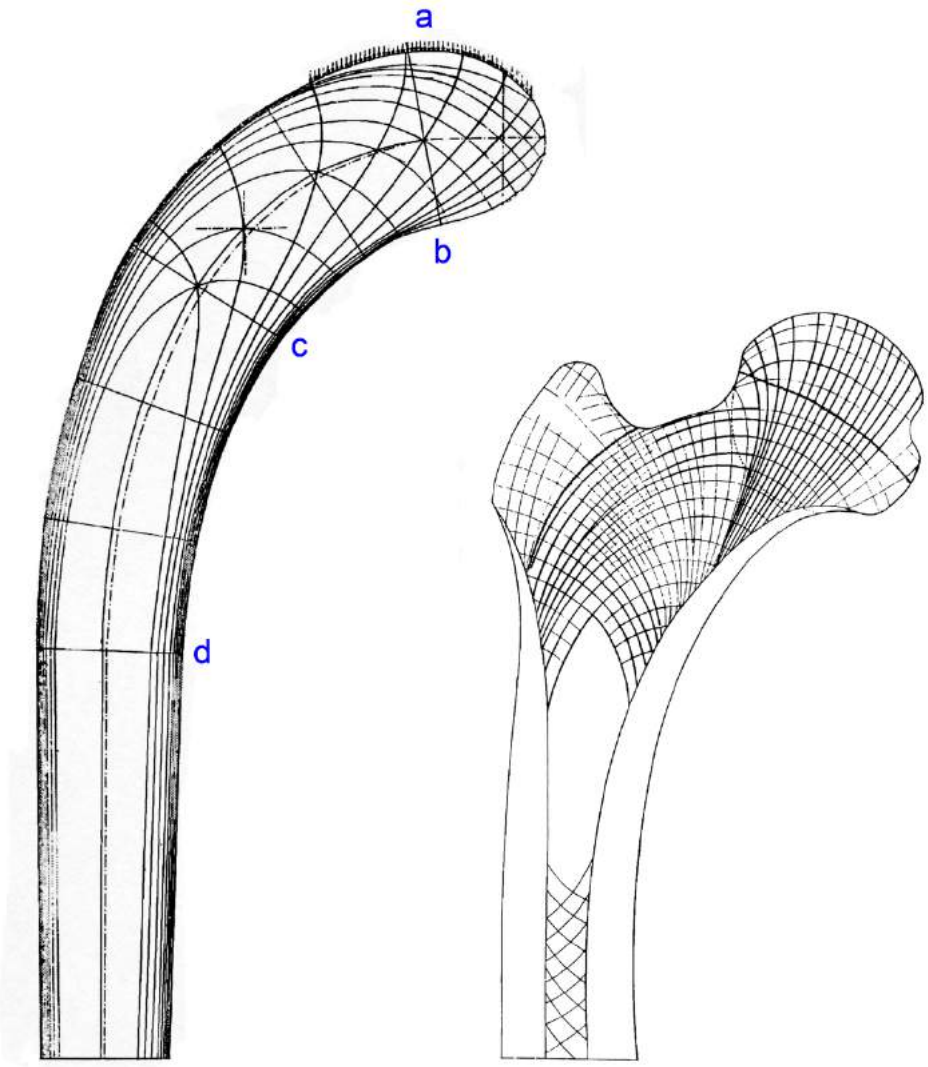

Figure 2 *Culmann´s compression lines of a Fairbairn crane (left) in comparison to the trabecular arrangement of the human proximal femur (right) as described by Julius Wolff.*

Following these observations, one can comprehend the stated fact that in bone formation, the femur is built in the most appropriate way possible. It used a minimum of material while having the ability to present sufficient stability for the mechanical demands and the attachment of the powerful muscles of the lower extremity.
Going one step further and moving away from this static demonstrations, Julius Wolff performed experimental modifications of the static stressing in animal models and used observations on pathologically altered biomechanical situations as they are seen in clump foot patients and described the following:

a) *"Restitution of a new appropriate overall shape of the bone…;*
b) *Resorption of previous trabeculae and formation of new trabeculae and plates of cancellous bone … adapted to the altered shape of the bone…;*
c) *Development of new cancellous areas with appropriate architecture and medullary cavities…; and*
d) *Formation of medullary cavities in the middle of cancellous bone."* ([7]; page 29)

These observations are the essentials for his theories of bone adaptation. Here, Julius Wolff states that not only the formation of bone is subjected to the applied mechanical load, but a change in load distribution essentially leads to a reconstruction to an optimal supportive structure.
Friedrich Pauwels, who continued Wolff´s research, reinforced his ideas in the 1980 published "Biomechanics of the locomotor apparatus". Pauwels for himself described bone as remodeling throughout life, undergoing a constant process of formation and resorption to determine and obtain a situation of "ideal stress". If the actual stress presents itself as larger as or smaller as the ideal situation, more bone is correspondingly formed or resorbed during the maintenance process. His findings lead to the conclusion that the "trajectorial arrangement of cancellous bone and its re-orientation when the stressing is altered appear as a forceful consequence of the principle of construction of the bone" [8].

1.2 Morphological parameters of functional adaptation within the Osteochondral Unit

The above described adaptational processes lead to an intimate relationship between form and function is perhaps nowhere as evident as in the musculoskeletal system. Here, the individual tissue arises as reaction to a given mechanical stimuli from undifferentiated embryonic tissue and forms a hierarchy of structural and kinematic harmony. The final organic form itself strongly supposes that specific features exist for specific reasons ("law of functional adaptation") which has been demonstrated through the analysis of the morphologic parameters within the osteochondral unit (OU) of synovial joints since it is known to be an integral and dynamic component that transmits and diverts the in- and out- coming forces through the joint [8, 9].

Within itself, the OU consists of the articular cartilage on top, the following tidemark as separation line towards the calcified cartilage which lays on top of the thin cortical lamella known as the subchondral bone plate (SBP) (Fig. 3) [10]. Its complex three-dimensional (3D) structure is due to the arrangement of sheets of parallel collagen fibrils which continue into the trabecular network of the spongy bone which form the basic framework for the embedded calcium hydroxyapatite. With its wave-like appearance, the SBP is known to be the mineralization front of the calcified cartilage, separating the cartilage and the subarticular spongiosa [11-13].

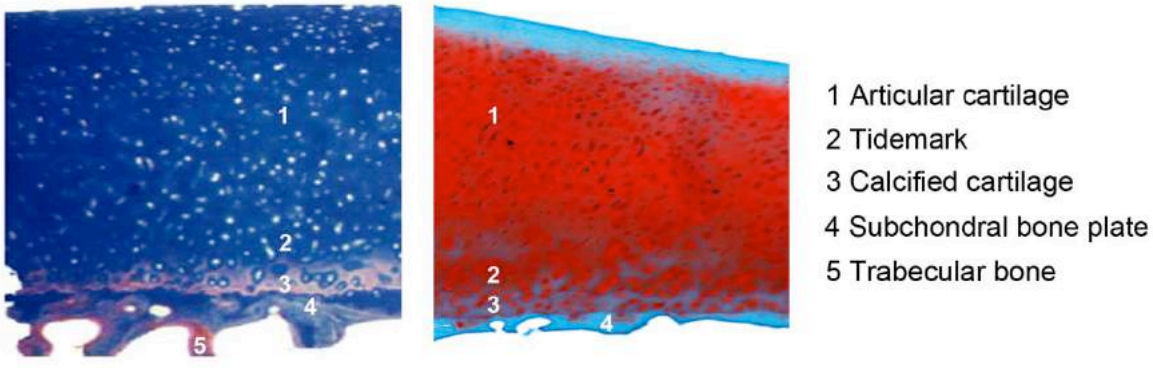

Figure 3 *Stained histologic sections of the Osteochondral Unit (with kind regards to the Institute of Anatomy, University of Basel).*

During the transmission process of incoming mechanical stress onto a joints surface, compressive, tensile or shearing stresses are created. They in their entirety define the crucial relationship between the long-term load intake and the morphology of the OU.

The external forces, depending on the extent of the local deformation, will lead to an increase or decrease of biologic material since the ability of an active response is given. As primary supportive tissue the articular cartilage and calcified cartilage react to the differences in incoming load with an adaptation of their regional thickness. One can say that the hyaline cartilage shows a greater thickness in a synovial joint in places where a greater load is applied onto the articular surface [14, 15]. Shepherd et al. even discussed a correlation of this cartilage thickness of the joints of the lower extremity to the body mass index. They showed that the larger and heavier a body is, the thicker the hyaline cartilage presents itself within the lower limbs [16].

Below these two parts, the SBP also holds pattern of a regular and reproducible structure. Regarding the thickness, current literature describes a high variability within and in-between joints. But, in general, convex shaped articular parts present a thinner SBP than the concave or flat counterparts [17, 18]. In case of the tibial plateau for example, it has been shown that the greatest thickness as located at the centre of the contact areas with a steady decrease towards the periphery. Furthermore, the SBP of the medial condyle, where 60% of the load is transferred, is significantly thicker than the one on the lateral condyle [19-21].

Next to the thickness, changes in long-term load intake cause integration and degradation of calcium hydroxyapatite within the collage framework in the SBP which generates distribution pattern of mineralization unique for each human and joint [13, 22, 23]. According to Pauwels, the distribution of mineralisation within the SBP of the OU is the reflection of the long-term stress intake of an articular surface and represents the loading history [14, 24, 25]. Altogether, areas with high mineralization resemble areas of high long-term load intake and, together with the regional differences in distribution, mirror the biomechanical demands of the SBP.

To analyse and display these pattern of density/mineral distribution, the method of computed tomography-osteoabsorptiometry (CT-OAM) was developed and described by Müller-Gerbl in 1998 [13]. Using conventional CT-Data, the method enables the display of the density distribution of the whole joint surface in a color-coded pattern and provides information about the long-term mechanical stimuli of the joint *in-vivo*.

Results obtained with this method show in accordance to the described thickness of the SBP within the tibial plateau the zone of greatest mineralization located on the medial condyle where under physiologic conditions 60% of the load are transferred. It is directly located beneath the contact point with the femoral counterpart [26] (Fig. 4a).

For the glenohumeral joint, a reproducible monocentric or bi-centric pattern was described on the concave glenoid. On the humeral head, matching locations of high density zones are found [27] (Fig. 4b).

Another newly conducted study on the human talus contributed to the theory of functional adaptation as well and described distribution pattern of mineral density in regards to the long-term load intake. As reported by Leumann et al., the biomechanical usage of the talar dome defines the anatomical structure and induces the mineralization within areas of high load intake [28] (Fig. 4c).

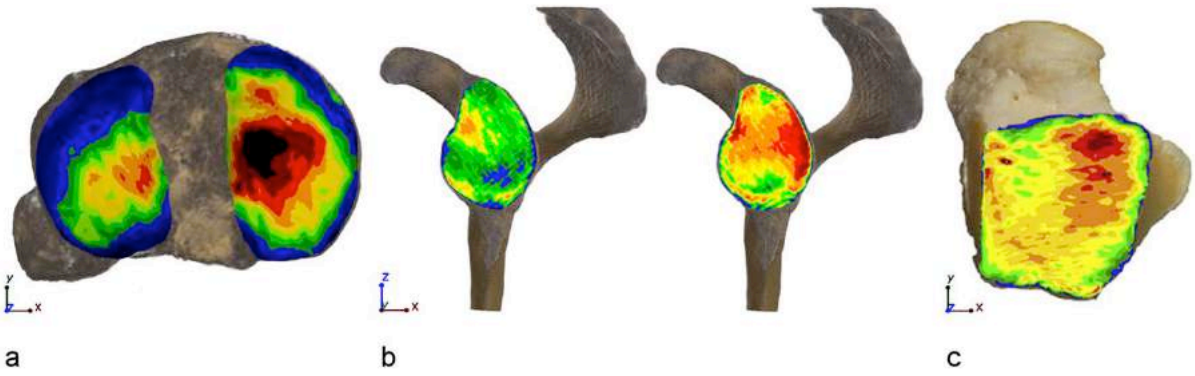

Figure 4 *Selected examples on density distribution pattern via CT-OAM.*
a. Tibial plateau, cranial view, left = lateral
b. Glenoid cavity, lateral view, left: monocentric pattern, right = bi-centric pattern
c. Talar dome, cranial view, left = medial

Continuing this work and analysing the architectural adaptations of long-term load intake of the deepest layer of the OU, Nowakowski et al. showed that the trabecular network below the SBP is built and adapted to achieve a maximum of support. In areas with high load intake, they found the most stable 3D-formation of trabecular bone, in areas with low load intake a significantly less supportive arrangement [29].

All these studies describe a regular and reproducible pattern of structural arrangements in accordance to the long-term load intake and suggest a strong correlation to the biomechanical situation of a joint.

The sensitivity towards a biomechanical stimulation or, respectively a change of the force transmission, has been impressively demonstrated by Müller-Gerbl in 1998, where patients with knee malalignment were in focus of the investigations of the SBP. In their study, they found differences in the tibial density distribution in accordance to the altered mechanical loading. I case of a genu valgum, the mineral concentration on the lateral

tibial condyle was considerably raised with an extended maximum while the mineralization of the medial condyle was greatly reduced. In the case of a genu varum malalignment, not only was the mineralization of the medial condyle increased, but its location was shifted to the medial edge. One year after correction osteotomy, control trials showed the displacement of position as well as the alteration in mineralization shifted significantly back to a distribution in accordance to physiological loading [30].
In this study, the functional adaptation, as it has been described by Julius Wolff and Friedrich Pauwels, was impressively demonstrated.

1.3 The biomechanics and known morphology of the human patella

As the largest sesamoid bone of the human body, the patella centralizes the divergent forces deriving from the 4 heads of the quadriceps muscle and increases their functional lever arm by transmitting the generated force across the knee to the patellar tendon and tibial tuberosity at a greater distance from the axis of rotation. In the movement of sliding along the femoral condyles, the hyaline articular cartilage provides an aneural and frictionless thick tissue that is specifically adapted to the bearing of high compressive loads [28, 31]. Additionally, it functions as a bony shield for the trochlea and the femoral condyles while the knee is in flexion [32].
Since the tibia rotates laterally during the knee extension process, the tibial tubercle, as the insertion point for the patellar ligament, becomes laterally displaced. The so created quadriceps angle between the line of application of the quadriceps force and the direction of the patellar tendon produces therefore a lateral displacement vector (resultant force = F_r; Fig. 5a) of the patella in the frontal plane [33]. In consequence, the contact area of the lateral patellar facet with the lateral femoral condyle within the patello-femoral joint (PFJ) is about 60% larger than on the medial side. The vector also leads to a consistently greater contact force on the lateral facet of the patella [34-37].
This biomechanical situation within the PFJ accounts for the specific anatomical structure of the knee cap as a response. As studies on physiologic human patellae revealed, a predominant maximum of density on the lateral facet of the articular surface of the patella can be found (Fig. 5b). The described maximum decreases peripherally but shows extensions over the vertical ridge in between both facets onto the medial side. Furthermore, Eckstein at al. [38] showed a constant maximum in cartilage thickness on the lateral facet which correlates with the described density distribution (Fig. 5c). These

regular and reproducible distribution pattern of both mineralization of the SBP and cartilage thickness can be seen as an adaption of the locomotor system of long-term load intake in regards to the ideas of Julius Wolff.

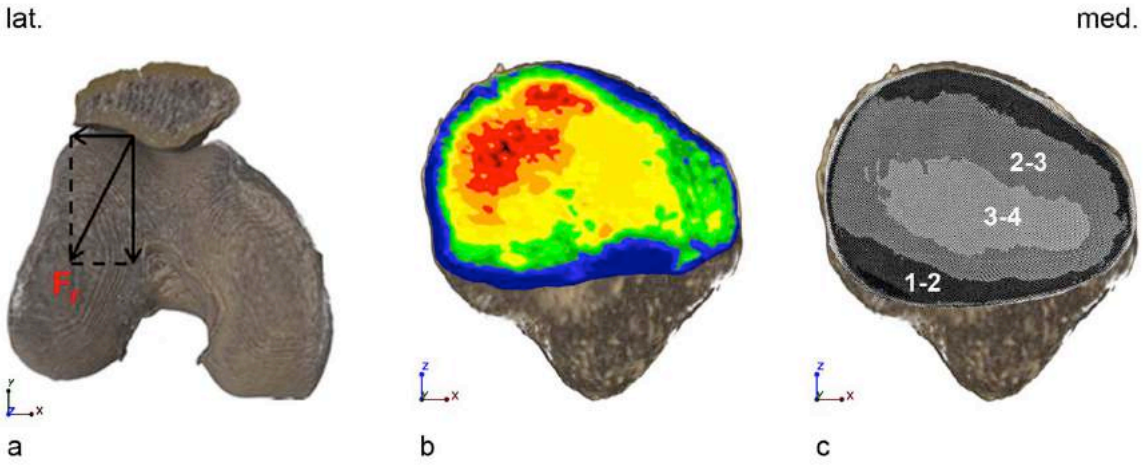

Figure 5 *Biomechanical situation of the PFJ.*
a: Right femur and patella in distal view, F_r = resultant force of lateral displacement
b: Patella, dorsal view, density distribution displayed via CT-OAM (in descending order: black, red, orange, yellow, green, blue)
c: Patella, dorsal view, cartilage thickness representation in adaptation of Eckstein et al. (in millimeter)

2 Aims of this work

Unlike other joints, the PFJ has only recently generated interest in the scientific community. Consequently, the knowledge about any physiological or pathological distribution of both, structural parameters as well as mechanical ones is still sparse.
In particular, the distribution of mechanical strength fields across the SBP and a method of evaluation in vivo will be of benefit for a better understanding of the long-term load distribution and the alteration through pathological processes. Regular load distribution could be evaluated, pathologies could be detected and an alteration process could be monitored over time.
Apart from the above-mentioned, the trabecular system of the patella has only been investigated on 2D cuttings and requires further investigation. Full detail about the 3D arrangement is still missing.
Of special interest is the trabecular arrangement in in dependence to the long-term load intake of the SBP. This way, it could be evaluated how the SBP distributes the load to

the inside of the bone and how areas of high and low load intake are structured as sign of adaptation.
The changes within the SBP and trabecular structure could provide conclusive information concerning OA of the PFJ and the pathological mechanism it initiates. So far it is understood that the properties of joint cartilage change as to maintain tissue homeostasis. Next to matrix remodelling, the cartilage adapts by cell proliferation and the pressure distribution is altered, however the mechanism of adaptation of the structures beneath the cartilage is not understood.

Therefore, we aim to investigate the Osteochondral Unit of the human patella and show that the anatomical architecture represents a direct adaptation to the loading history.
The three main investigations will include:

- the analyses of mechanical properties of the SBP in regards to its density distribution;

- the investigation of the subarticular bone for its structural and numerical parameters of trabecular network; and

- the changes occurring in above mentioned systems in degenerated samples.

3 Outline of this thesis

This thesis is the outcome of a cumulative 4 year study about the adaptation of anatomical characteristics in regards to the mechanical influences and analyses the sequential expression of bony properties of the SBP as well as the trabecular network on a historical record of the “loading history.

The publications arising combine the methods of medical imaging analysis via CT- and micro-CT as well as mechanical testing.

(*i*) While the first aspect examines a visually displayed density distribution of the SBP in regards to its strength field distribution measured via indentational testing,

(*ii*) the second publication focuses on the distribution of the mechanically adapted trabecular bone beneath the subchondral bone plate.

(*iii*) In a last study, we will compare the generated information to a sample population which is altered due to degenerative effects and show classified sign of OA.

Chapter 4 discusses the extent of the Osteochondral Unit and the adaptation to the long-term load intake. It is shown, how highly differentiated the system remodels and reveals a congruency towards the biomechanics of the patello-femoral joint. In addition, changes in the homeostasis due to osteoarthritic changes are explained.

This thesis is completed by a conclusion as well as an outlook on the importance of the cellular level of bone in *Chapter 5*.

All analysis focused on the human patella where sparse information is available and which is of rising surgical and orthopedically interest.

The anatomical structures under investigation where chosen in consecutive order from the whole bone to a microscopic level and where published in pear reviewed journals. The submission criteria was the journals aim of structural level analysed.

4 Publications arising from this thesis

4.1 Density and strength distribution in the human subchondral bone plate of the patella

Sebastian Hoechel (1), Dieter Wirz (2,3), Magdalena Müller-Gerbl (1)

(1) Institute of Anatomy, University of Basel, Switzerland
(2) Laboratory of Biomechanics & Biocalorimetry, University of Basel, Switzerland
(3) Bruderholzspital, Basel, Switzerland

International Orthopaedics (SICOT), 2012
DOI 10.1007/s00264-012-1545-2

- ***Aim:*** *Identifying the topographical density distribution as described in literature for every individual patella and analysing the mechanical strength field distribution within the SBP to find possible correlations and link the mechanical strength to the long-term load uptake.*

Hypothesis:

- As described for the density distribution of human patellae, the strength field distribution is also not of homogenous nature;
- Areas of high density will be areas of highest strength;
- There is a correlation between density and strength field distribution within the whole of the SBP that allows us to draw direct conclusions from density to strength; and
- High long-term load intake triggers bony tissue to react with an increase in strength.

Experimental Approach:

To address this question, we performed a cross-sectional study of 10 pairs of healthy human patellae (Outerbridge classification: grade 0). Using the method of CT-OAM, we displayed the density distribution of the SBP and acquired density values (Hounsfield-

units) at predefined measuring points (ANALYZE 8.1, Biomedical Imaging Resource, Mayo Foundation, Rochester, USA). In collaboration with the Laboratory of Biomechanics & Biocalorimetry, University of Basel, indentation tests were performed on all samples at the corresponding measurement points. For comparison of results, we generated two-dimensional (2D) distribution charts based on our measuring grid system for visual comparison. Finally, the displayed data was evaluated using regression analysis.

Outcome:

The analysis showed density distribution pattern with a localized maximum of density on the lateral facet, decreasing concentrically. As for the mechanical strength distribution, we found similar results, which are in correlation to the density distribution (r^2 = 0.89 - 0.97; Ø 0.92). The results demonstrate that the SBP as dynamic component transmits forces through the joint and therefore adapts to its mechanical needs. The known theories of stress distribution through the patello-femoral joint are in strong agreement with the density and strength distribution pattern. It was shown that areas of high long-term load transmission increase their density by osteoblastic deposition of calcium hydroxyapatite and therefore also increase the mechanical strength. A statistically significant direct relationship of strength and density links both morphological parameters and therefore allows conclusions from one to the other.

International Orthopaedics (SICOT)
DOI 10.1007/s00264-012-1545-2

ORIGINAL PAPER

Density and strength distribution in the human subchondral bone plate of the patella

Sebastian Hoechel &Dieter Wirz &
Magdalena Müller-Gerbl

Received: 24 February 2012 / Accepted: 4 April 2012

Abstract
Purpose The aim of this study was to map the strength distribution of the human patella and correlate it to the subchondral bone plate density obtained by means of computed tomographyosteoabsorptiometry (CT-OAM).
Methods Measurements were performed at 34 standardized points on each patella. The mineralization patterns of the subchondral bone plate of 20 patellae were displayed with the help of CT-OAM. False-coloured distribution patterns for our measurements were generated. The mechanical strength was determined at the same points by indentation testing.
Results We showed that neither the density nor the mechanical strength is distributed homogeneously but exhibited regular, reproducible distribution patterns which mirror long-term stress distribution in articular surfaces. A direct correlation was found between both parameters in the subchondral bone plate.
Conclusion The correlation of density and mechanical strength makes CT-OAM a valuable tool to assess and monitor changes in the strength of the subchondral bone plate in vivo.

S. Hoechel · M. Müller-Gerbl (*)
Institute of Anatomy, University of Basel,
Basel, Switzerland
e-mail: m.mueller-gerbl@unibas.ch

D. Wirz
Laboratory of Biomechanics & Biocalorimetry,
University of Basel,
Basel, Switzerland

Introduction

The patellofemoral joint (PFJ) consists of the articulation surfaces of the patella and the distal, anterior femur, as well as the surrounding soft tissue structures. Complaints in this anterior compartment of the knee are reported to have a one-year prevalence of 20–25 % with an increased proportion among athletes [1, 2]. Reasons for this so-called patellofemoral pain syndrome (PFPS) are abnormal tracking of the patella or increased pressure on the patellofemoral joint surfaces, generated by a malalignment of the lower extremity, patellar malalignment, or muscle imbalance [3, 4].

Patients usually describe the pain as highly disabling with a huge impact on work and daily life routine. With the increase in sports activities in today's lifestyle, it is likely the number of incidents will rise.

PFPS treatment covers a wide variety of surgical procedures like tibial tuberosity transfer, lateral retinacular release, trocheoplasty or sagittal osteotomy of the patella after Morscher. The biomechanical changes in alignment of the quadriceps muscle, the patella and the patellar tendon improves the use of cartilage by enlarging the area of surface contact taking pressure, the nutrition of the cartilage due to a greater contact area of patella and femur and

Published online: 01 May 2012

reduces the intramedullary pressure to lower or eliminate pain [5–8].

To understand the changes occurring within the bony structures of the joint, which is initiated by realignment procedures, one has to understand the biomechanics of the knee joint and the functional architecture of the patella. Due to the external rotation of the tibial tuberosity in maximal extension of the knee, the Q-angle is maximized and the lateral facet of the patella has the most contact area with the femur condyle. The medial facet comes into contact with the femur from 20° flexion. Throughout the flexion towards 90° the contact area is shaped like a narrow band, crossing the articulation surface horizontally. Flexion towards 135° shows a change in contact pressure. Here, the medial facet lies free and only the proximal part of the lateral facet as well as the odd facet engage the femur [7, 9]. During knee flexion, the lateral surface has greater contact area than the medial one, suggesting a higher load bearing capacity for the lateral surface [10].

Since it is well established that the mechanical stimuli received over a long period of time adapt the passive locomotor system and remodel it for optimal distribution of the forces transmitted through it, the anatomy of the articulation surface of the two patella would be expected to be highly variable [11, 12]. Previous data showed differences in cartilage thickness, thickness of the subchondral bone plate, and in density distribution of the subchondral bone plate throughout the joint surface [13, 14].

The uncalcified cartilage covering the patellar articulation surface has a maximum thickness of up to 5 mm in the middle of the lateral facet. The cartilage shows a wider distribution of this thickness in the medial to lateral direction than proximal to distal. From this centre it decreases concentrically to the periphery. The thickness of the underlying subchondral bone plate also follows a regular distribution pattern, having its maximum thickness on the lateral facet, with a general range from 100 μm to 1000 μm, sometimes even exceeding 2000 μm, and falling off towards the periphery [14].

Concerning the distribution of the density within the subchondral bone plate of an articular surface, the non-invasive technique of computed tomography osteoabsorptiometry (CT-OAM) provides information on differences in relative distribution [15]. Unlike usual methods of CT densitometry, which allow measurements of absolute values for bone density in large areas, here the relative distribution is demonstrated over the whole joint surface in a false-colour diagram [16]. Using this method, Eckstein et al. [13] described the maximum density of the subchondral bone plate of the human patella to be constantly localized on the lateral surface, which also supports the previous results on patellar architecture.

All these findings describe regular and reproducible distribution patterns of structural properties in the human patella, which can be seen as an adaption of the locomotor system to long-term stress of the articulation surface [11–13, 15]. In order to provide information about the mechanical properties of the subchondral bone plate in relation to its density, we topographically map the mechanical strength of the subchondral bone plate of the patella and correlate our findings with the density distribution. Knowing the maximal contact area, thickness of the subchondral bone plate and density to be mainly on the lateral facet, we expect the maximal mechanical strength to be on the lateral facet as well. We hypothesize that it will highly correlate with its density distribution. If so, CT-OAM will not only show the distribution of density values, but also will give information about the actual strength of the subchondral bone plate. In clinical routine, this information could be used to identify joint parts with a pathological increase of long-term stress intake and to monitor changes in the joint structures after surgical procedures.

Material and methods

Preparations

This study included ten pairs of frozen human patellae, which were obtained from the Department of Pathology (University of Basel, Switzerland), obtained from ten body donors (five male, five female; aged 61–92, average 81 years).

CT-scans (Siemens Somatom Sensation 64 CT Scanner, 1 mm slice-thickness) of each sample were performed in cooperation with the Department of Radiology (Kantonsspital Bruderholz, Basel, Switzerland).

Photographic documentation of the samples was done separately for the lateral and medial facet. Due to the tilt of these two surfaces, we documented both sides in horizontal view and fused the images into one whole picture. With respect to the average size of the patella, the oval shape and the minimum distance of the indentation measuring points needed to ensure the subchondral bone plate did not break. Therefore, we developed a 34-point coordinate system for CT-OAM and indentation testing. The measuring grid was size-independent and projected digitally on the fused image of every sample (Fig. 1).

Density distribution patterns generated by CT-OAM

For the following CT-OAM analysis, we loaded the CT datasets into ANALYSE 8.1 (Biomedical Imaging Resource, Mayo Foundation, Rochester, USA) for visualization and measurement [17]. Using this program, we produced a 3D reconstruction of each patella in two different views. In the first reconstruction, we horizontally showed the lateral facet and in a second one the medial

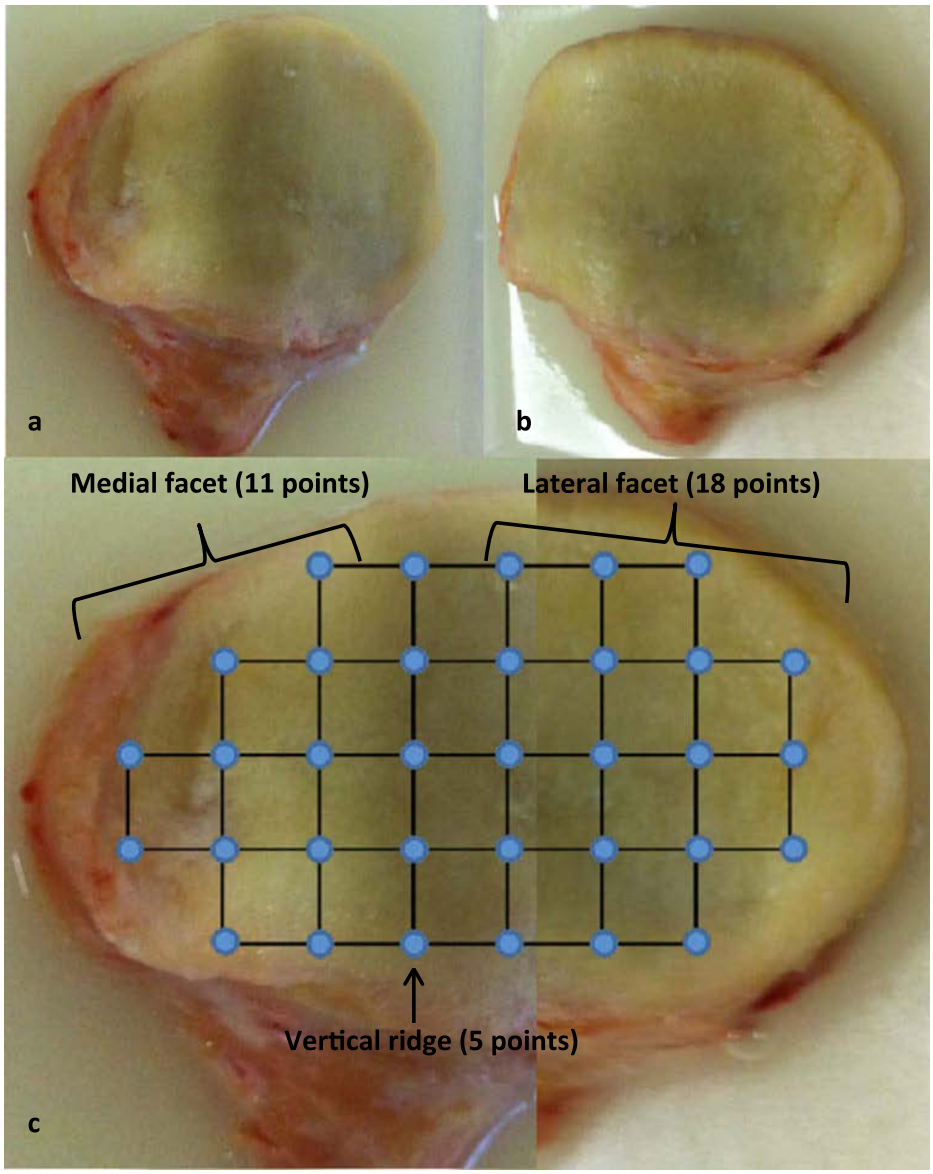

Fig. 1 Right human patella. **a** Medial facet in plain view. **b** Lateral facet in plain view. **c** Fused image overlaid by coordinate system with 34 measuring points for indentation testing (sample S-4)

facet. In the end, we fused both datasets into a combined volume. In a second step, we isolated the subchondral bone plate of the patellae manually in every CT-image for a "maximum intensity projection". This way, for every single image point, the maximum density value of the underlying bone plate is projected onto the top surface. By classifying the Houndsfield units (HU) into steps of 100 HU and assigning them to false colours, we displayed the density distribution of the subchondral bone plate of the human patella in a diagram. To determine exact localization of the density values to be measured, we superimposed the coordinate system onto the density pattern of the 3D reconstructed patella (Fig. 2).

Indentation testing

Ligamental and soft tissue structures attached to the patellae were removed. The cartilage, covering the subchondral bone plate, was also manually removed. For attachment to the indentation machine we cemented the patellae in poly(methylmetacrylate) (PMMA). It was possible to rotate them using a ball-bearing to position the test point perpendicular to the indentation needle. Afterwards, we identified the measuring points regarding the digital coordinate system on the 3D reconstructions of the patellae. To determine the mechanical strength by indentation, an indentation test machine (Synergie 100, MTS Systems, 2 kN loadcell) was used. A steel needle

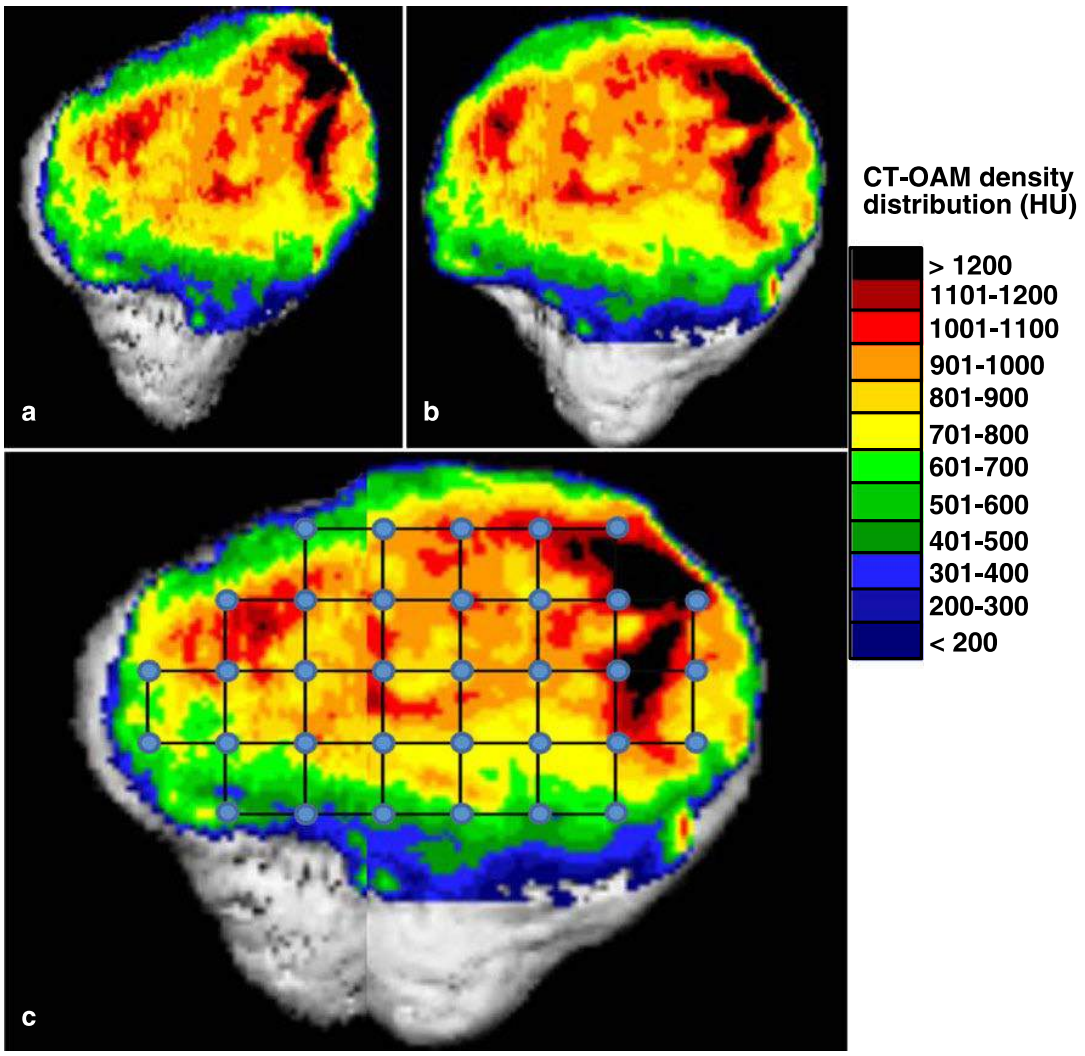

Fig. 2 CT-OAM density distribution image of the right human patella. **a** Density distribution pattern of the medial facet. **b** Density distribution pattern of the lateral facet. **c** Fused image with measuring points for density values (sample S-4)

(ø=1.3 mm) created a standardized hole of 7 mm (1 mm/sec) at every measuring point. The penetration forces of all 34 identified points for each patella was plotted against time by the computer and tabulated. The maximum strength needed during indention testing for every measuring point of the patella was identified and recorded. Visualization of the force distribution was done in a standardized grid system.

Density-strength correlation

To compare the density values and the mechanical strength values, we measured the density (HU) for every corresponding indentation measuring point on the CTOAM distribution chart. We scaled the dataset to 8-bit and determined the value according to the 34 measuring points of our coordinate system with the help of ANALYSE 8.1. The recorded data was visualized in standardized grid system according to indentation data.

The recorded data of mechanical strength and subchondral density was examined by linear regression (Fig. 3).

The Pearson product–moment correlation was determined for all measured samples. Using a two-tailed t-test, we statistically analysed the significance of the correlation ($P<0.01$).

Results

Density of the subchondral bone plate

Our results revealed that the density of the subchondral bone plate of the human patella is not distributed homogeneously. The maximum values of 19 samples were consistently found on the lateral facet with only one sample where the highest density values were situated on the medial facet. Originating at the localization of the highest density, values showed to

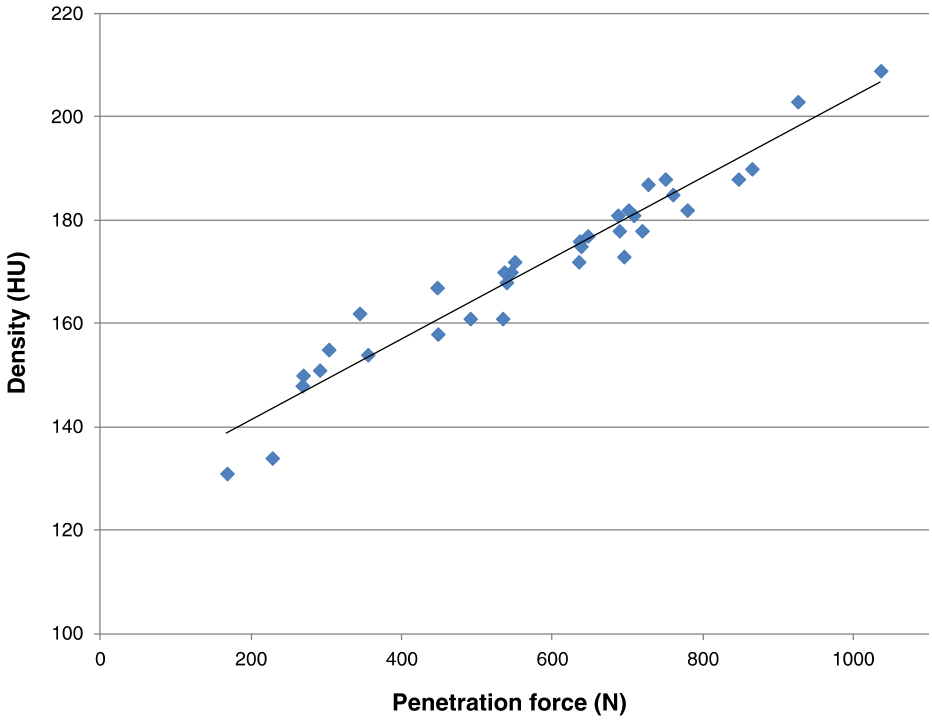

Fig. 3 Distribution of correlation of density values and penetration force values of sample S-4 (r^2=0.97)

fall off towards the periphery (Fig. 4a, b, e, and f). The density maxima showed an interindividual range between 163 HU and 199 HU.

Mechanical strength of the subchondral bone plate

The mechanical strength distribution of the subchondral bone plate tested by indentation revealed similar distribution patterns as CT-OAM did. Again, strength maxima were located in 19 samples on the lateral facet, once on the medial facet, falling off to the periphery.

Interindividual differences in mechanical strength have been seen; the minimum force needed to penetrate the subchondral bone plate was shown to be below 30 N in the periphery, reaching 1034 N in areas with highest density (Fig. 4c and g).

Mineralization-strength correlation

Visual comparison of the density distribution patterns and the distribution of penetration force values already showed strong similarities. In every sample, the patterns of density distribution and the mechanical strength distribution showed that the point of maximum is on the same facet and localization. A direct correlation between the determined density values and the penetration force values of all measuring points was found for every sample (Fig. 4d and h). The coefficient of correlation (r^2) ranged from 0.89 to 0.97 (mean 0.92) and was statistically significant ($p<0.01$) (Table 1).

Discussion

The generated density distribution charts localized the maximum in density of the subchondral bone plate of the human patella mainly on the lateral facet, decreasing concentrically. This result was expected and matches previous studies that show similar distribution patterns with the lateral facet bearing the region of maximum bone density [13, 18]. The one exception in our analysis, showing the maximum density to be on the medial facet, is mainly due to a malalignment and unusual pressure distribution as can be seen by the severe cartilage damage on the joint surface.

Compared with former reports of pressure transmission through the PFJ, the localization of the density maxima appears to be where the maximum area of contact and generated pressure is situated. The reason for that is the tension of the quadriceps muscle, which increases considerably in knee flexion [19, 20]. Considering the subchondral bone to be a dynamic component that transmits forces through a joint and adapts to its mechanical need, the known theories of stress distribution through the PFJ are in strong agreement with the density distribution patterns. Areas of long-term high load transmission increase the density of the subchondral bone plate by osteoblastic

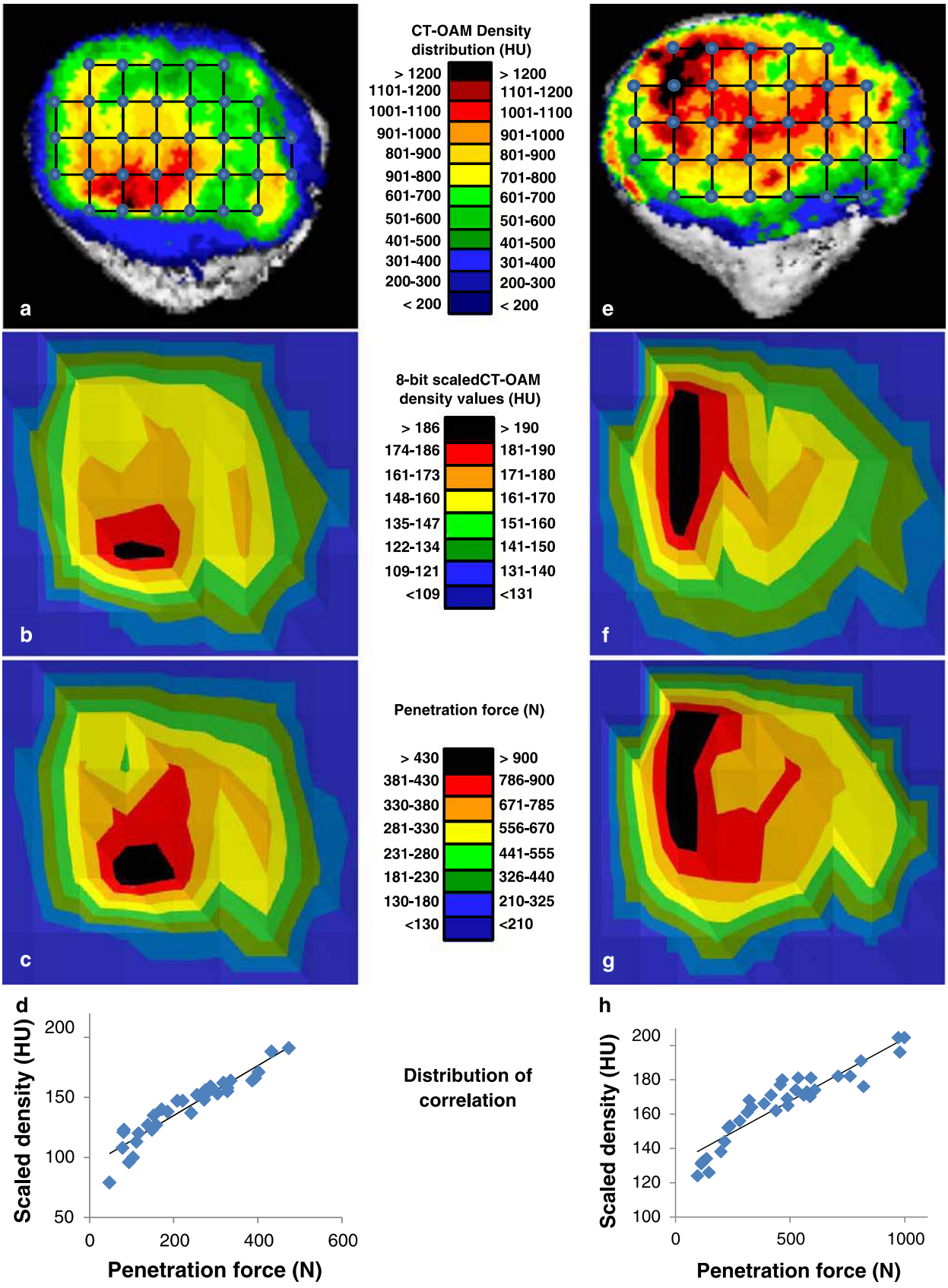
a
CT-OAM Density distribution (HU)
> 1200
1101-1200
1001-1100
901-1000
801-900
901-800
601-700
501-600
401-500
301-400
200-300
< 200
> 1200
1101-1200
1001-1100
901-1000
801-900
701-800
601-700
501-600
401-500
301-400
200-300
< 200
e
b
8-bit scaledCT-OAM density values (HU)
> 186
174-186
161-173
148-160
135-147
122-134
109-121
<109
> 190
181-190
171-180
161-170
151-160
141-150
131-140
<131
f
c
Penetration force (N)
> 430
381-430
330-380
281-330
231-280
181-230
130-180
<130
> 900
786-900
671-785
556-670
441-555
326-440
210-325
<210
g
d
Scaled density (HU)
200
150
100
50
0
200
400
600
Penetration force (N)
Distribution of correlation
h
Scaled density (HU)
200
180
160
140
120
100
0
500
1000
Penetration force (N)

◀ **Fig. 4** Correlation of density and penetration force of two representative samples [S-13 (**a**–**d**) and S-3 (**e**–**f**)]. **a**, **e** Density distribution pattern generated by CT-OAM, overlaid by the coordinate system for the location of the 34 defined points for the simultaneous measurements of density and force values. **b**, **f** Visual representation of density values at measurement points, HU scaled to 8-bit. **c**, **g** Visual representation of penetration force values at measuring points. **d**, **h** Distribution of correlation for density values (HU, 8-bit scaled) and penetration force (N)

calcium deposition and the density distribution finds its maximum here [21, 22].

For mechanical properties such as the strength of the subchondral bone plate in correlation to the density distribution, recent studies provide data about the inferior tibial facies and the glenoid cavity. Here, a direct correlation between these two parameters can be seen [13, 23, 24]. These authors imply clinical use of density distribution patterns generated with CT-OAM to determine subchondral bone quality for optimal screwing positions in orthopaedic endoprotheses. Our results on the subchondral bone plate of the human patella also state a high correlation between the density and the mechanical strength. The correlation clearly states that the density distribution patterns of human patellae generated by the means of CT-OAM also describe its mechanical strength. Apparently, we can see the density distribution throughout the subchondral bone plate of a joint as a parameter of long-term load intake which results in osteoblastic calcium deposition and leads to a correlating increase in strength.

Changes in the loading history of a joint could therefore be visualized and monitored in vivo with CT-OAM. If, in surgical procedures, the loading of the PFJ is changed in order to treat PFPS, the effect of the procedure on the PFJ and the changes occurring in the subchondral bone plate could be analysed in vivo to monitor the outcome and to follow-up the result.

Conclusion

Since the subchondral bone plate in a diarthrodial joint is a dynamic component, it adapts to its mechanical needs generated by work, sports or daily routine. Areas exposed to long-term high load transmission increase in density.

The density distribution in the subchondral bone plate of the human patella gives not only information about the mineralization by osteoblastic calcium deposition, but also correlates to its mechanical strength and therefore is a parameter for the long-term load distribution through the articular surfaces of the PFJ.

The correlation of density distribution and mechanical strength makes CT-OAM a useful tool to determine the strength distribution of the subchondral bone plate in vivo as well as analyse and monitor changes over time.

Disorders in shape, size, and the resulting differences in contact area and pressure distributions could be diagnosed

Table 1 Clinical and statistical data of the specimens

Specimen	Age (years)	Gender	Side	8-bit density (HU)	Penetration force (N)	r^2
S-1	63	M	Left	111–164	66–420	0.93
S-2	63	M	Right	114–185	62–565	0.93
S-3	91	M	Left	124–199	113–999	0.92
S-4	91	M	Right	131–209	168–1034	0.97
S-5	91	M	Left	112–197	57–550	0.97
S-6	91	M	Right	113–181	84–531	0.92
S-7	66	M	Left	126–178	65–427	0.89
S-8	66	M	Right	111–175	30–481	0.93
S-9	61	M	Left	130–199	131–830	0.93
S-10	61	M	Right	118–195	95–722	0.92
S-11	88	F	Left	122–181	39–494	0.90
S-12	88	F	Right	111–164	23–236	0.93
S-13	83	F	Left	96–191	79–474	0.94
S-14	83	F	Right	101–197	70–516	0.94
S-15	86	F	Left	124–199	55–538	0.96
S-16	86	F	Right	111–193	55–624	0.92
S-17	92	F	Left	113–164	83–316	0.89
S-18	92	F	Right	111–170	39–370	0.89
S-19	89	F	Left	110–195	50–618	0.90
S-20	89	F	Right	121–186	54–521	0.90

M male, *F* female

as well as monitored after surgical procedures. The effect of realignment procedures on the PFJ can be assessed in follow-up studies to visualize the changes in load transmission.

References

1. Outerbridge RE (1961) The etiology of chondromalacia patellae. J Bone Joint Surg Br 43-B:752–757
2. van Middelkoop M, van Linschoten R, Berger MY, Koes BW, Bierma-Zeinstra SM (2008) Knee complaints seen in general practice: active sport participants versus non-sport participants. BMC Musculoskelet Disord 9:36. doi:10.1186/1471-2474-9-36
3. Malek MM, Mangine RE (1981) Patellofemoral pain syndromes: a comprehensive and conservative approach. J Orthop Sports Phys Ther 2(3):108–116
4. Puddu G, Giombini A, Selvanetti A (2001) Rehabilitation of sports injuries: current concepts. Springer, Berlin, New York
5. Christoforakis J, Bull AM, Strachan RK, Shymkiw R, Senavongse W, Amis AA (2006) Effects of lateral retinacular release on the lateral stability of the patella. Knee Surg Sports Traumatol Arthrosc 14(3):273–277. doi:10.1007/s00167-005-0699-5
6. Feller JA, Amis AA, Andrish JT, Arendt EA, Erasmus PJ, Powers CM (2007) Surgical biomechanics of the patellofemoral joint. Arthroscopy 23(5):542–553. doi:10.1016/j.arthro.2007.03.006
7. Fulkerson JP, Hungerford DS, Ficat RP (1990) Disorders of the patellofemoral joint, 2nd edn. Williams & Wilkins, Baltimore
8. Pecina M, Ivkovic A, Hudetz D, Smoljanovic T, Jankovic S (2010) Sagittal osteotomy of the patella after Morscher. Int Orthop 34 (2):297–303. doi:10.1007/s00264-009-0923-x
9. Ahmed AM, Burke DL, Yu A (1983) In-vitro measurement of static pressure distribution in synovial joints. Part II: retropatellar surface. J Biomech Eng 105(3):226–236
10. Salsich GB, Ward SR, Terk MR, Powers CM (2003) In vivo assessment of patellofemoral joint contact area in individuals who are pain free. Clin Orthop Relat Res 417:277–284. doi:10.1097/01.blo.0000093024.56370.79
11. Pauwels F (1965) Gesammelte Abhandlungen zur funktionellen Anatomie des Bewegungsapparates. Springer-Verlag, Berlin, New York
12. Wolff J (1986) The law of bone remodelling. Springer-Verlag, Berlin, New York
13. Eckstein F, Muller-Gerbl M, Putz R (1992) Distribution of subchondral bone density and cartilage thickness in the human patella. J Anat 180(Pt 3):425–433
14. Milz S, Eckstein F, Putz R (1995) The thickness of the subchondral plate and its correlation with the thickness of the uncalcified articular cartilage in the human patella. Anat Embryol (Berl) 192 (5):437–444
15. Müller-Gerbl M (1998) The subchondral bone plate. Advances in anatomy, embryology, and cell biology, vol 141. Springer, Berlin, New York
16. Muller-Gerbl M, Weisser S, Linsenmeier U (2008) The distribution of mineral density in the cervical vertebral endplates. Eur Spine J 17(3):432–438. doi:10.1007/s00586-008-0601-5
17. Muller-Gerbl M, Putz R, Hodapp N, Schulte E, Wimmer B (1990) Demonstration of subchondral density pattern using CT-osteoabsorptiometry (CT-OAM) for the assessment of individual joint stress in live patients. Z Orthop Ihre Grenzgeb 128(2):128–133. doi:10.1055/s-2008-1039487
18. Tillmann B, Brade H (1980) Die Beanspruchung des Femoropatellargelenks. Anat Anz 147:477–478
19. Maquet P (1976) Biomechanics of the knee. Springer, Berlin, Heidelberg, New York
20. Scuderi GR (1995) The patella. Springer, New York
21. Ficat RP, Hungerford DS (1977) Disorders of the patello-femoral joint. Williams & Wilkins, Baltimore
22. Minns RJ, Birnie AJ, Abernethy PJ (1979) A stress analysis of the patella, and how it relates to patellar articular cartilage lesions. J Biomech 12(9):699–711
23. Gordon KD, Duck TR, King GJ, Johnson JA (2003) Mechanical properties of subchondral cancellous bone of the radial head. J Orthop Trauma 17(4):285–289
24. Kraljevic M, Zumstein V, Wirz D, Hugli R, Muller-Gerbl M (2011) Mineralisation and mechanical strength of the glenoid cavity subchondral bone plate. Int Orthop 35(12):1813–1819. doi:10.1007/s00264-011-1308-5

4.2 Insight into the 3D-trabecular architecture of the human patella

Sebastian Hoechel (1), Georg Schulz (2), Magdalena Müller-Gerbl (1)

(1) Department of Biomedicine, Musculosceletal Research, University of Basel, Pestalozzistrasse 20, 4056 Basel, Switzerland
(2) Biomaterials Science Center, University of Basel, Schanzenstrasse 46, 4056 Basel, Switzerland*

**Supported by the Swiss National Science Foundation (Grant 316030_133802/1)*

Annals of Anatomy, 2015
DOI 10.1016/j.aanat.2015.02.007

Motivation:

In literature, this expression of “Wolff’s law” was incipiently discussed by Ficat and Hungerford in 1977 [39]. They described the sheets of trabecular bone as more or less parallel to each other but perpendicular to the coronal plane of the patella and therefore slightly oblique vis-à-vis the articular facets. The described results are interpreted as an architectural behavior in dependence to the applied tensile forces and to ideally meet the mechanical demands. At about the same time, Raux et al. also worked on the trabecular architecture of the human patella [40]. Their analysis of microradiographs, derived from sagittal and horizontal cuts, went one step further and firstly described a sheet-and-rod model. Here, orientated sheets of bony tissue which accounted for trabeculae were connected laterally by rods. The lamellae on the lateral facet are described to be more parallel and orientated than on the medial one, which, in its systematic manner, is descripted as response to the biomechanical demands of the patella.

Considering these cornerstones of trabecular analysis, I tried to go one step further.

- ***Aim:*** *Taking the Evaluation of structural parameters one step further and analysing the 3D-architecture of the trabecular network below the SBP of non-pathological human patellae with regards to the long-term load intake of the patello-femoral joint as it is mirrored in the density distribution of the SBP.*

Hypothesis:

- Structural and numerical parameters of trabecular architecture will vary between the lateral and the medial facet of the patella;
- They as well will show differences in distribution throughout each articular surface and also vary in function of the distance to the SBP; and
- The trabecular architecture will resemble an adaptation to the long-term load intake in way to optimally support the SBP in a matter of “form follows function” as described by Julius Wolff.

Experimental Approach:

For this study on non-pathologically altered human patellae (Outerbridge classification: grade 0), 10 isolated samples were evaluated. After assessing the density distribution of the SBP via the method of CT-OAM, the sample collection was scanned with a phoenix nanotom® m for research and industrial requirements using
3D-metrology to create 3D-reconstructions of the samples. To assess the parameters of architecture of these reconstructions, a cascade of software system was used. The visualization and measurement software VGStudio® Max 2.2 (Heidelberg, Germany) was used to predefine regions of interest, MATLAB® (MathWorks, Natick, Massachusetts, U.S.A) to binary datasets, and Skyscan™ CT-analyser (Skyscan N.V., Aartselaar, Belgium) to calculate the architectural parameters of interest.
The resulting data was visualized and statistically evaluated.

Outcome:

The arrangement and architecture of the trabecular varied strongly throughout the trabecular system of the patella. Across the articular surface, each parameter was distributed distinctively. Parameters resembling a strong supportive arrangement showed a maximum on the lateral facet where parameters describing a weak arrangement showed a minimum. These pattern were consistent throughout the evaluated depth-steps down to 5 millimetres below the SBP but consistently lessened in intensity. The correlation to the density distribution (BV/TV: $r^2 > 0.81$; Tb.N: $r^2 > 0.88$; Tb.Th.: $r^2 > 0.79$; DA: $r^2 < -0.76$; and SMI: $r^2 < -0.75$) was significant ($p < 0.05$).
The results clearly support the hypothesis that the trabecular network, in its function to support the SBP, adapts to its mechanical needs according to the long-term load intake of the PFJ.

In addition to the 3D-measurements, the simulation of 2D-measurements of the same datasets reveals systematic differences. The quantification of these divergences gives conclusive evidence that certain parameters are measured lower and others are overstated in previously described 2D-measurement data found in literature.

Annals of Anatomy 200 (2015) 98–104

Contents lists available at ScienceDirect

Annals of Anatomy

journal homepage: www.elsevier.de/aanat

Research article

Insight into the 3D-trabecular architecture of the human patella☆

Sebastian Hoechel[a,*], Georg Schulz[b], Magdalena Müller-Gerbl[a]

[a] Department of Biomedicine, Musculoskeletal Research, University of Basel, Pestalozzistrasse 20, 4056 Basel, Switzerland
[b] Biomaterials Science Center, University of Basel, Schanzenstrasse 46, 4056 Basel, Switzerland

ARTICLE INFO

Article history:
Received 13 October 2014
Received in revised form 19 January 2015
Accepted 5 February 2015

Keywords:
Human patella
Subchondral bone plate
Long-term load intake
Trabecular architecture
Micro-computed tomography

ABSTRACT

The subchondral bone plate (SBP), a dynamic component of the osteochondral unit, shows functional adaptation to long-term loading by distribution of the mineral content in a manner best serving the mechanical demands. Since the received joint-load is transmitted into the trabecular system, the spongy bone also exhibits differences in strain energy density which models it for optimal support. To evaluate the regional variations in trabecular architecture, in accordance with the density distribution of the SBP revealing its long-term load intake, CT- and μCT-datasets of ten physiologic patellae were analysed for defined parameters of bony structure. For the SBP, the density distributions as well as area measurements were used. The trabecular architecture was described using parameters of bone morphology comprising the first 5 mm (examined in 1 mm steps) below the SBP. The obtained measurements are: Bone volume fraction (BV/TV); Bone surface density (BS/TV); Trabecular number (Tb.N); Trabecular separation (Tb.Sp); Trabecular thickness (Tb.Th); structure model index (SMI); and the Degree of anisotropy (DA). The evaluated architectural parameters varied within the trabecular system and showed an inhomogeneous distribution pattern. It proved to be distinctive with maxima of material and stability situated below areas of the highest long-term load intake. With increasing depth, the pattern of distribution was persistent but lessened in intensity. The parameters significantly correlated with the density distribution of the SBP within the first and second millimetres. With increasing depth down to the fifth millimetre, the coefficients of correlation decreased for all values. The trabecular network adapts to its mechanical needs and is therefore not homogenously built. Dependent upon the long-term load intake, the trabecular model optimizes the support with significant correlation to the density distribution of the SBP.

1. Introduction

In recent years the concept of "bone's functional adaptation", often referred to as "Wolff's Law" (Wolff, 1892), has been described in literature based on the research on the osteochondral unit (OCU) of the human patella. The mechanical stimuli initiating this adaptation process are the resultant forces on the posterior patellar surface in accordance with its biomechanics.

As the largest sesamoid bone, the patella increases the functional lever arm of the quadriceps muscle by transmitting the generated forces across the knee to the tibial tubercle at a greater distance from the axis of rotation. Additionally, it centralizes the divergent forces of the quadriceps muscle and acts as a link between the quadriceps tendon and the patellar ligament. Since the tibia rotates laterally during the knee extension process, the tibial tubercle becomes laterally displaced as it is the insertion point for the patellar ligament. The remaining quadriceps angle (Q angle) between the line of application of the quadriceps force and the direction of the patellar tendon produces a lateral displacement vector of the patella on the frontal plane (Fox et al., 2012). In consequence, the lateral facet contact area is about 60% greater than the medial one which leads to a consistently greater contact force on the lateral side (Hehne, 1990; Hefzy et al., 1992; Hefzy and Yang, 1993; Fitzpatrick et al., 2011; Borotikar and Sheehan, 2013).

Following this biomechanical situation within the patellofemoral joint (PFJ), the OCU of the patella shows general signs of adaptation to the distribution of the long-term load intake. The articular as well as the subchondral bone plate (SBP) show their largest expansion on the lateral facet, with the SBP also having its maximum density and mechanical strength situated

☆ Supported by the Swiss National Science Foundation (Grant 316030_133802/1).
* Corresponding author. Tel.: +41 0 61 267 39 37.
E-mail address: sebastian.hoechel@unibas.ch (S. Hoechel).

http://dx.doi.org/10.1016/j.aanat.2015.02.007
0940-9602/

here (Eckstein et al., 1992; Milz et al., 1995; Eckstein et al., 1998; Hoechel et al., 2012).

Connected to the supporting trabecular network just below, the OCU distributes and transmits the generated strain and long-term load intake of the PFJ into this network of spongy bone and towards the anterior cortical bone of the patella.

Due to its stabilizing effect beneath the SBP, the trabecular network has increasingly become a subject of scientific interest due to its remodelling abilities. Following the idea that the trabecular architecture is arranged along the lines of the pressure it has to bear and, in this way, provides the most effective support, Humphry, as one of the first scientists to study this network, described the trabecular architecture of the proximal femur in 1858 (Humphry, 1858). Culmann and later Wolff compared these findings to an industrial crane design (Fairbairn crane) and first defined a dependency of trabecular lining to the direction of pressure generated within the human skeleton (Wolff, 1892).

For decades after, these findings on trabecular architecture were understood to be physiologic optimization to maintain integrity while minimizing bone mass. Naturally, numerous studies investigated the effects of anisotropy, connectivity as well as morphologic parameters of this network. As for the patella, the first architectural model was established in the mid-1980s by Raux and Townsend. They developed a basic model consisting of plates and interconnecting rods, which filled the space between the SBP and the dense anterior cortical bone. The most important findings document that the arrangement of trabecular differs within the patella and that zones of horizontal sheets with single axis orientation can be differentiated from zones of mixed orientation (Raux et al., 1975a,b; Townsend et al., 1976). Substantiated insights were later provided by Toumi et al., who demonstrated that the trabecular architecture varies in a complex manner between the lateral and medial facet. Their analysis of longitudinally sectioned patellae shows a significantly greater number of trabeculae orientated antero/posteriorly in the medial and central parts of the bone than laterally. Obliquely and medial–lateral orientated trabeculae were homogenously distributed in all areas of the bone. The transversely sectioned patellae revealed significantly more antero/posteriorly orientated structures in the medial and central parts, with the most obliquely aligned trabeculae were located on the lateral facet (Toumi et al., 2006a,b). Even though the analyses were performed using two-dimensional (2D) measurement techniques, the results provide remarkable insights, in having demonstrated the variation in the trabecular architecture of the patella. In addition, they reported differences in bone volume fraction between the patellar facets (Toumi et al., 2012). Unfortunately, a dependency of the internal architecture and the existing joint forces of the PFJ cannot be investigated using these methods and still remains unclear.

To investigate the theory of "form follows function" and to link the pressure distribution within the PFJ to the inside architecture of the patella, we used the established method of computed tomography osteoabsorptiometry (CT-OAM) to describe the long-term load intake of the SBP according to its density distribution. We interpreted the results in respect to the analysed 3D trabecular architecture beneath (Muller-Gerbl et al., 1989; Hoechel et al., 2012). The aim of our study is to evaluate the trabecular architecture below the SBP and describe the distinctive distribution pattern for every analysed parameter. The development of the architecture in depth will give an insight into trabecular adaptation to maintain a balanced stress level. In addition, we attempt to draw conclusions about the dependency of architectural parameters on the individual long-term load intake of the SBP.

Since the method of CT-OAM is based on conventional CT-data, the dependency of results on the CT-OAM and the trabecular architecture could be used to draw conclusions about the trabecular network in clinical routine.

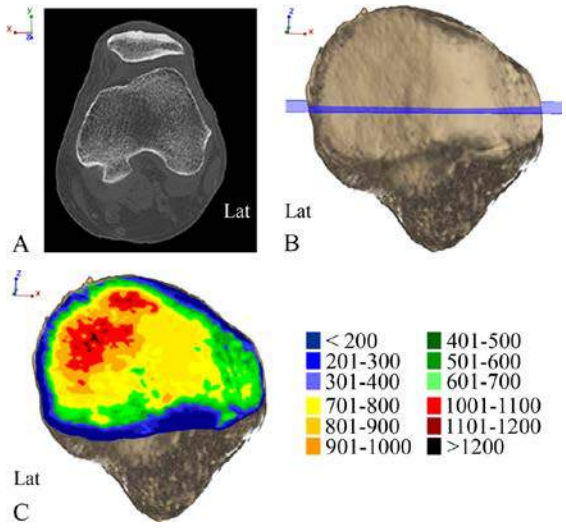

Fig. 1. Method of CT-osteoabsorptiometry of the human patella (A). Axial CT-image of a left knee (B). Isolated 3D reconstruction of the patella (posterior view), axial plane (of A) marked in blue (C). Density distribution of the subchondral bone plate of the patella including caption (in Hounsfield Units [HU]). (For interpretation of the references to color in this figure legend, the reader is referred to the web version of this article.)

2. Materials and methods

2.1. Material

A total of 10 human patellae (4% formalin concentration, fixed over 48 h, Outerbridge classification: Grade 0), acquired from donors to the Institute of Anatomy, University of Basel, Switzerland, were used. The sample population included 5 male and 5 female patellae (age 65–78, mean 72; 6 right samples, 4 left). All donors contributed their body to research at the University of Basel, Switzerland.

2.2. Methods

2.2.1. Density distribution of the SBP via CT-OAM

The CT-data required to display the density distribution in relationship to the mineralization of the SBP were generated on a conventional CT-scanner (SOMATOM 16, Siemens, Erlangen, Germany, 120 kilovolt [kV], 180 milliampere-second [mA s], slice thickness 0.6 millimetre [mm], axial slices) at the Institute of Anatomy, University of Basel, Switzerland. The CT-datasets were evaluated using the image analysing software ANALYZE® 11.0 (Biomedical Imaging Resource, Mayo Foundation, Rochester, MN, USA). After isolating the SBP of the patella, a 'maximum-intensity-projection algorithm' analysed the density distribution within. As a result, the densest voxels in posterior–anterior direction were projected onto the top of the SBP and assigned to a colour-chart where the most dense voxels (1200 Hounsfield Units [HU]) were designated black, lower values red, yellow, green and blue (in descending order, steps of 200 HU). Afterwards, the resulting image was projected onto a 3D reconstruction of the patella for anatomical orientation. The final models, representing the long-term loading history through the density distribution of the whole joint surface of the patella, served as a basis for further investigation (Fig. 1) (Muller-Gerbl et al., 1989, 1990; Muller-Gerbl, 1998; Hoechel et al., 2012).

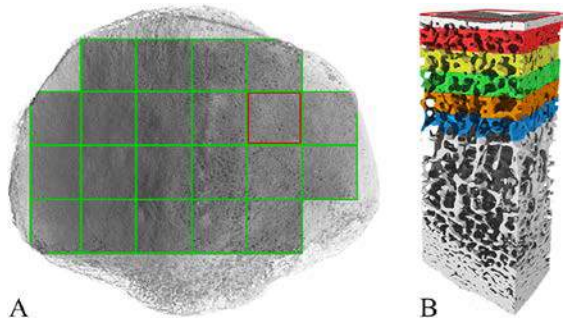

Fig. 2. Method of μ-CT; definition of measurement cube and regions of interest. (A) 3D reconstruction, left patella in dorsal view, 21 areas for extraction of measurement cubes marked. (B) Measurement cube with 5 highlighted regions of interest (1st ROI: red; 2nd ROI: yellow; 3rd ROI: green; 4th ROI: orange; 5th ROI: blue) just below the subchondral bone plate. (For interpretation of the references to color in this figure legend, the reader is referred to the web version of this article.)

2.2.2. Micro-computed tomography for evaluation of trabecular architecture

The phoenix nanotom® m is a nanoCT® system for research and industrial requirements using a 3D metrology. It creates 3D reconstructions of cross-section scans from objects up to 300 mm in diameter with voxel sizes down to 1 micrometre (μm). All samples were scanned equally using this cone-beam device with micro-focus tube, acceleration voltage 140 kV, at a beam current of 60 mA s. In addition, a 0.5 mm aluminium filter was used to minimize beam hardening. Each scan included 2100 projections from 360 degrees. The resulting isotropic voxel size of the generated images accounted for 32 μm. The nanotom® m reconstruction of the 3D dataset is based on a modified Feldkamp algorithm which integrated the patella fractions into one 3D object (Feldkamp et al., 1984).

With the help of VGStudio® Max 2.2 (Heidelberg, Germany), each 3D dataset was virtually divided into 21 measurement cubes. Cube measurements: proximal-distal: 8 mm, lateral–medial: 8 mm, posterior–anterior: SBP to the anterior cortical bone. The remaining odd measurement cubes were neglected since here the SBP is not supported by trabeculae of any kind as it is in direct contact with the anterior cortical bone (Fig. 2).

On every measurement cube, the first five mms of trabecular bone just beneath the SBP were divided into five, equally sized ($8 \times 8 \times 1$ mm) regions of interest (ROI). 1st ROI: 0–1 mm of trabecular bone just below the SBP, 2nd ROI: 1–2 mm of trabecular bone below the SBP, likewise for the 3rd, 4th, and 5th ROI (Fig. 2B). Measurements of trabecular architecture were performed equally on all ROIs for all cubes with the help of the Skyscan software CT-analyser® (Bruker-Microct, Belgium).

2.2.3. Obtained parameters for analysis

In accordance with the literature and the described main parameters of trabecular bone architecture:

(a) BV/TV (%), Bone volume fraction
(b) BS/TV (1/mm), Bone surface density
(c) Tb.Th (mm), Trabecular thickness
(d) Tb.Sp (mm), Trabecular separationas primary measurements in bone histomorphometry (Hildebrand et al., 1999).
Derived indices:
(e) Tb.N (1/mm), Trabecular numberas structural parameter (Parfitt et al., 1987; Hildebrand et al., 1999). As well as:
(f) SMI (dimensionless), Structure model index
(g) DA (dimensionless), Degree of anisotropyto directly quantify the otherwise subjective classification of plate-like and rod-like trabecular architecture and to assess the 3D symmetry of it (Hildebrand and Ruegsegger, 1997).

For evaluation, the data of the ROIs of the measurement cubes was assigned to five layers and represented in 2D distribution charts. Therefore, every assessed parameter of the 1st ROIs was reassembled in one layer, stating the distribution of this parameter across the articular network of the patella. Likewise the data was arranged down to the 5th ROIs of all measurement cubes (fifth layer) (Fig. 3).

In addition to these trabecular data, the mean density (HU) of the SBP of every measurement cube was derived from the density distribution charts compiled via CT-OAM. The results were tabulated and assigned to the corresponding trabecular dataset.

2.2.4. Statistics

For all appraised samples, the Pearson product-moment correlation coefficient was established. Using a two-tailed *t*-test, the significance was performed. For analysis of data distribution, the Kolmogorov–Smirnov test was used. All statistical analyses were done using RStudio (RStudio: Integrated-development environment for R, Version 0.96.122, Boston, MA, USA).

3. Results

3.1. Density distribution of the SBP via CT-OAM

The results showed the peak density area to be consistently located on the lateral facet. Originating at this localization of highest density, a steady decrease was found towards the periphery. Density values recorded on the medial facet have a considerably lower absolute value (Fig. 1, representative sample). The maxima on the lateral side, however, showed substantial inter-individual differences. The peak values of the maxima varied from 928 HU to 1411 HU, lowest density values of all samples ranged from 282 HU to 658 HU.

3.2. Parameters of trabecular bone

(a) BV/TV, (b) BS/TV; within the 2D distribution charts, the distribution of bone and bone surface density is inhomogeneous in every analysed layer (Fig. 3). Consistently, maxima of bone volume and surface density are found beneath the lateral facet, decreasing into the periphery. The medial facet shows significantly ($p > 0.05$) lower values. The pattern of distribution reveals a consistency into depth, where the parameters show a peak on the lateral facet as well. The range of maximum and minimum values gradually decreases with depth as the distribution becomes more homogenous.

The decrease of bone volume and bone surface density with every layer of depth is visualized in Fig. 4.

(c) Tb.Th, (e) Tb.N; again, the maxima of these parameters are found below the lateral facet, with values decreasing into the periphery. The pattern also showed consistency down to the 5th mm (Figs. 3 and 4).

(d) Tb.Sp; the trabecular separation differs across the trabecular architecture as well but proved to have a persistent minimum below the lateral facet, representing packed stacks of trabecular bone. The highest values, interpreted as loose formation of trabecular are found below the medial facet and in the periphery (Fig. 3). Overall, highest and lowest values found within the 1st layer increasing with depth (Fig. 4).

(f) SMI; within the analysed sample population, we found plate-like trabecular mainly below the lateral facet. Rod-like architecture was seen below the medial part and in the periphery. The pattern of

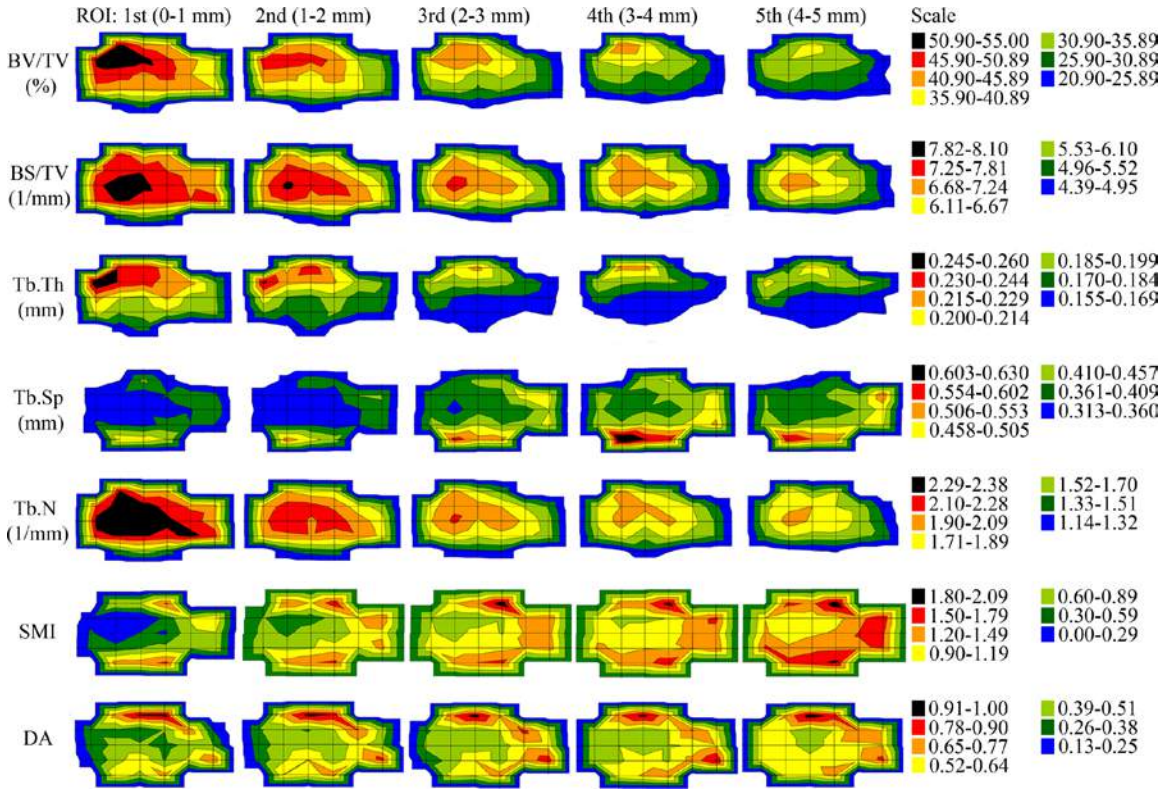

Fig. 3. 2D distribution charts of trabecular architectural parameters for the five analysed ROIs from the first to the fifth millimetre (same sample and orientation as Fig. 2).

Table 1
Mathematical description of the dependency of trabecular parameters of the human patella and the according depth (1st to the 5th ROI) as presented in Fig. 4.

Parameter	Dependency of (x) and (y)	Correlation*
BV/TV	$y = -8.76\ln(x) + 37.05$	$r^2 = 0.99$
BS/TV	$y = -1.03\ln(x) + 6.65$	$r^2 = 1.00$
Tb.Th	$y = -0.02\ln(x) + 0.19$	$r^2 = 0.98$
Tb.Sp	$y = 0.07\ln(x) + 0.36$	$r^2 = 1.00$
Tb.N	$y = -0.34\ln(x) + 1.91$	$r^2 = 1.00$
SMI	$y = 0.35\ln(x) + 0.76$	$r^2 = 1.00$
DA	$y = 0.03\ln(x) + 0.53$	$r^2 = 0.98$

(x) = depth below the subchondral bone plate (mm), (y) = parameter value.
* Correlation of logarithmic dependency to measured mean values (Fig. 4).

distribution continued down to the 5th layer (Fig. 3), the absolute values of the SMI increased (Fig. 4).

(g) DA; we found an area of isotropic constellation below the lateral facet within the 1st layer of ROIs, which changed into a more anisotropic state with depth. The medial part as well as areas in the periphery showed higher values expressing a more anisotropic state that increased with depth. The distribution pattern persisted down to the 5th layer with the differences between maximum and minimum reducing gradually (Fig. 3). The overall anisotropy increased with depth (Fig. 4).

The overall change in absolute values of every parameter (Fig. 4, y-axes) that occurs with depth (Fig. 4, x-axes) shows a logarithmic dependency (Table 1).

3.3. Trabecular bone parameters in correlation with density distribution of the SBP

Positive correlation coefficients were found for BV/TV, BS/TV, Tb.Th, and Tb.N. These parameters showed the highest correlation within the 1st analysed layer (r^2 up to 0.81). Down to the 5th layer, there was a steady decrease to $r^2 = 0.25$ (Table 2).

The Tb.Sp, SMI, and DA described a high negative correlation. Values of up to $r^2 = -0.82$ for the 1st layer also steadily decreased with depth down to values as low as $r^2 = -0.29$ in the deepest evaluated layer (Table 2).

4. Discussion

The idea of bony tissue not being rigid and inflexible is not new in literature. First publications describing the phenomenon of bone adaptation to imposed mechanical loadings can be found as early as in the 19th century, when shortly after, the femoral head was described as “highly motivated” by Karl Culmann and the ideas at that time were summarised and substantiated by Wolff (1892) and Bourgery (1854). The cornerstone of his work is the interpretation of the internal alignment of the trabeculae. Following along the principal stress directions expected from functional load bearing, the pattern of the trabecular framework is described as ‘controlled’ by the direction of the load acting onto the bone. Wolff further proposed that the orientation of trabeculae is transformable with alterations in loading pattern. His hypothesis and rules of transfiguration are still known as “Wolff’s Law” today (Wolff, 1892). Since then, the methods of macroscopic analysis and the in vitro assessment of bony structures developed towards a microscopic level. Thin section analysis, acquired either by sawing or cutting, is currently the most established method to describe and quantify structural parameters of trabecular bone. The disadvantages of these long-established methods are the interpretation of 2D sections and the use of mathematical models for extrapolation to

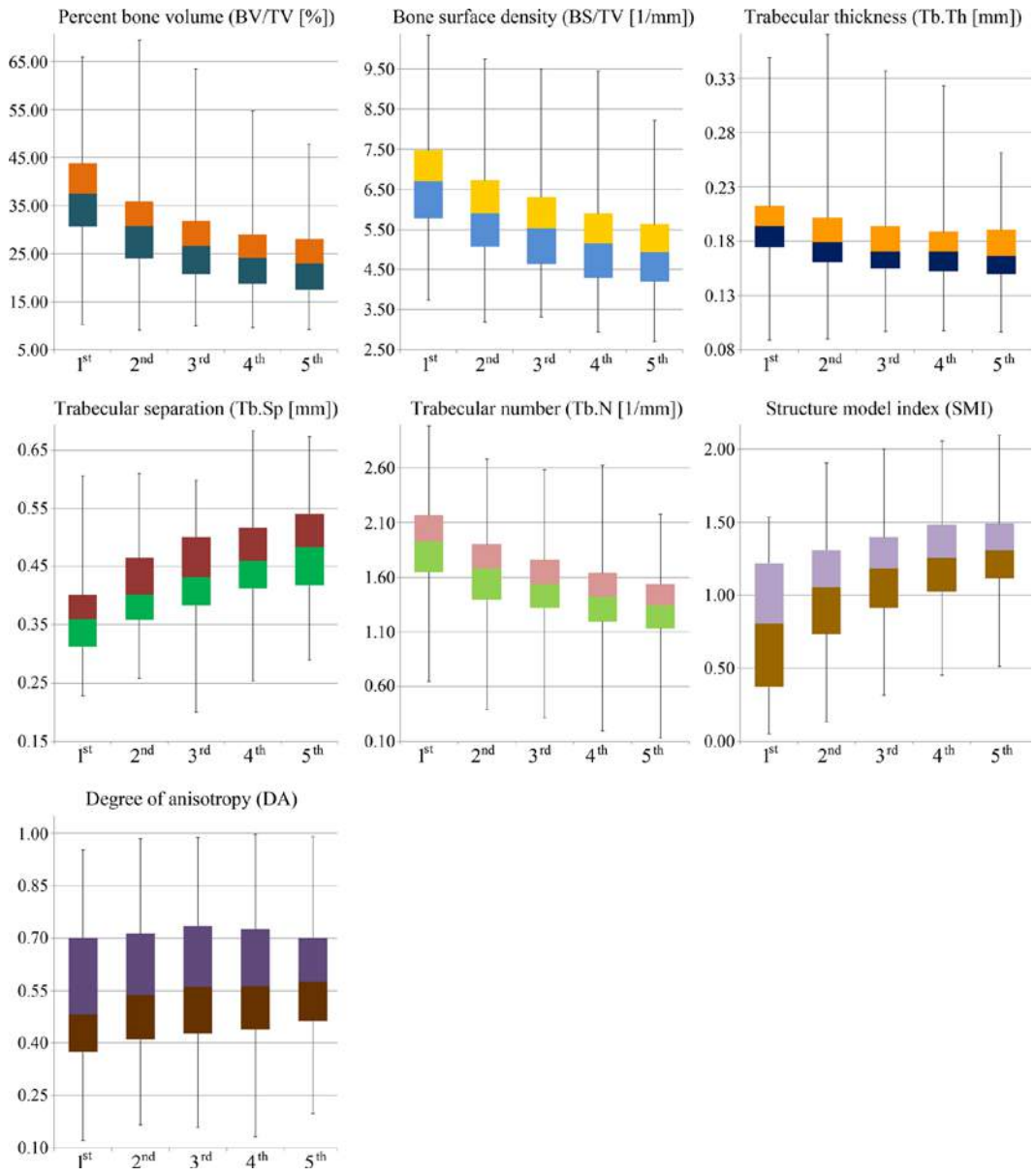

Fig. 4. Box-and-whisker plot of the development of the architectural parameter values of the trabecular network from the 1st to the 5th ROI below the subchondral bone plate of all samples (whiskers representing one standard deviation above and below the mean of the data).

Table 2
Trabecular bone parameters in correlation to density distribution of the SBP.

mm	BV/TV	BS/TV	Tb.Th	Tb.Sp	Tb.N	SMI	DA
0–1	0.81 (0.06)	0.81 (0.06)	0.73 (0.08)	−0.70 (0.10)	0.76 (0.13)	−0.82 (0.10)	−0.71 (0.05)
1–2	0.74 (0.09)	0.74 (0.11)	0.55 (0.14)	−0.55 (0.19)	0.63 (0.29)	−0.68 (0.26)	−0.65 (0.12)
2–3	0.62 (0.14)	0.62 (0.18)	0.44 (0.14)	−0.49 (0.26)	0.59 (0.27)	−0.56 (0.24)	−0.56 (0.12)
3–4	0.49 (0.19)	0.49 (0.23)	0.32 (0.22)	−0.54 (0.16)	0.58 (0.21)	−0.50 (0.29)	−0.46 (0.14)
4–5	0.44 (0.18)	0.44 (0.22)	0.25 (0.21)	−0.24 (0.33)	0.48 (0.22)	−0.39 (0.33)	−0.29 (0.18)

(. . .) = standard deviation.

the 3D arrangement which consistently lead to false assumptions (Engelke et al., 1999).

Today, microcomputer tomography presents an emerging alternative to histomorphometry. Time-consuming preparation like cutting, staining, or radiologic analysis of serial sections is redundant and the analysis is of direct character without interpolation based on mathematical models and the assumption of the 3D architecture. Since the initial technical limitations improved greatly, it is possible to evaluate complete bones and describe the architecture of the whole 3D trabecular network at once. As for the patella, we were able to map the architecture of the trabecular network below the whole articular surface and directly represent it.

The biomechanics of the PFJ are mainly influenced by the setting of the extensor mechanism using the patella as a pulley. Being the focus for the insertions of the large quadriceps muscle at its top, the patella also serves as an insertion point for the patellar ligament at its base. Together, the applied forces acting on the small mobile bone with an incongruent geometry lead to large contact stress (Amis and Farahmand, 1996). As the knee flexes and the patella slides into the trochlear groove, the patellofemoral contact initiates at the distant pole and moves upwards with increasing flexion (Aglietti et al., 1975). Due to the valgus angulation between the resultant line of action of the quadriceps muscle and the patellar tendon, the resultant force is directed against the lateral margin of the femoral trochlea (Hehne, 1990). This way, the greater area of contact is located on the lateral facet of the patella where the peak strain is also situated (Goodfellow et al., 1976; Scuderi, 1995; Fitzpatrick et al., 2011). With increasing extension, the peak strain on the patella moves in a distal and medial direction, always staying on the lateral facet (Borotikar and Sheehan, 2013). Adapting to this pressure transmission, the articular cartilage and the SBP beneath are known to show the maximum thickness, density, and strength here (Eckstein et al., 1992; Hoechel et al., 2012). The SBPs density distribution of the human patella can therefore be regarded as representing the long-term loading history (Muller-Gerbl et al., 1989; Muller-Gerbl, 1998).

The analysis of the trabecular architecture just below the SBP revealed structural properties in accordance with the biomechanical situation represented. It was not at all surprising that the parameters of BV/TV, BS/TV, Tb.Th, and Tb.N showed maxima just beneath the regions of maximal density in the SBP, which describe an accumulation of bone in order to maximize the support here. The reported maxima decreased into the periphery and showed less trabecular bone in the region of the patellar ridge and the medial facet just like the density distribution. Interestingly, these distribution patterns of trabecular bone are found to be consistent in the analysed depth of the trabecular system. Showing significant lower overall levels in the deeper layers, the distribution with maxima beneath the densest area is found down to the fifth millimetre. Next to this quantitative support, the parameters resembling the structure revealed the most stable arrangement beneath zones of highest load intake. The SMI described primarily a plate formation here, which changed into rods in the periphery. The DA of these trabecular indicates the most interconnections in between the plates whereas the periphery with less long-term load intake is designed with unconnected rods. The arrangement of the trabecular therefore shows not only the most material but also the strongest arrangement just beneath areas of highest load intake. Its arrangement is a direct result of mechanical input forming a distinctive architectural pattern in order to support the SBP in an optimal compromise of structure and material use.

Following high correlations of trabecular architectural parameters to the density distribution of the SBP within the first and second mm of analysed trabecular bone, the resulting force seems afterwards to be spread within the trabecular system in such a way that the inhomogeneous structure distribution with high differences of absolute values gradually becomes more homogenous, the differences in absolute level decrease and the correlation to the distinctive long-term load intake of the SBP lessens.

The described structural properties can be interpreted following the "Mechanobiology hypothesis" of Carter and Beaupré (Carter, 1984; Carter et al., 2007). Next to the biological component (r_b) of the genetic disposition of bone which is dominant during the juvenile growth period, the mechanical (r_m) component models bone in a way to experience optimum strain levels. This described strain energy density (SED) within the trabecular network is the summation of single load intake moments which is defined as "loading history" over a period of time where the differences in SED distribution over the articular surface seem to administer the delicate differentiation of each structural parameter. The trabecular adaptation changes from a high degree of differentiation just beneath the SBP to a more equal distribution within the lower analysed layers. This in the end creates a state of homeostasis between structural arrangement and equally distributed SED. But it is more than probable, that bone cells respond more to components of their mechanical environment than just physical deformation by the generated strain.

On a cellular level, the in vivo loading always triggers a fluid flow within the widely spaced lacunae interconnected by canaliculi. The produced oscillatory fluid flow results in a cell response via streaming potentials, chemo-transport and wall shear stress. The latter is believed to stimulate cell wall processes causing cell deformation and subsequent metabolic activity (Jacobs et al., 1998; Lanyon and Skerry, 2001; Wang et al., 2004).

The resulting trabecular architecture stimulated by these processes is therefore in strong correlation to the load and strain distribution of the articular surface. The forces transmitted from above form the network towards a distinct, optimally supportive architectural pattern as shown in this work. The spreading and absorption of these forces on their way into the depth of the trabecular network leads to an equalization of this network, once the distribution is homogeneous. This development can be mathematically accessed for every single parameter. The calculations and results presented are specifically for the patella and for a physiological condition only.

The data in this work concretises the previously described architectural arrangement of different plate orientations and differences in quantity of bony material across the trabecular network observed from 2D slices (Raux et al., 1975a,b; Townsend et al., 1975, 1976). Differences to the data observed by above mentioned authors as well as by Toumi et al. (2006a,b) result in the areas observed. In contrast to their research including the anterior trabeculae close to the cortical bone, we intentionally focussing on the trabeculae within the first 5 mm below the SBP with direct pressure intake through the joint.

With the help of μCT analysis of these trabeculae which receive the unaltered joint-pressure distribution via the SBP, the directly approached link of the biomechanics of the single patella through analysis of the long-term load intake in union with the trabecular structure can be approached. It reveals the highly differentiated architecture as a result of adaptation to optimize the support and strain distribution. The adaptations, generated by osteocytes in dependency on their local load and strain intake, can altogether advance the understanding of the form-function relation.

Even though the data describes the coherence of the above-mentioned structures, information about bone remodelling on a cellular level cannot be provided using μCT. In order to interpret the presented data for the forming and reabsorption of trabecular bone, histochemical and immunohistochemical demonstration of alkaline phosphatase activity of the subchondral bone will be performed. Since it has been suggested that subchondral

bone remodelling plays an important role in the progression of osteoarthritis where the exact pathogenesis still remains unclear, we will include osteoarthritic samples in the upcoming studies to compare to this data (Van den Berg, 2011).

Acknowledgements

Sebastian Hoechel and Magdalena Müller-Gerbl designed the study. Georg Schulz developed the technical implementation and supervised the use of the phoenix nanotom® m. Sebastian Hoechel collected the data, developed the methodology, and wrote the manuscript.

We kindly thank the Swiss National Science Foundation for their financial support with the acquisition of the phoenix nanotom® m (R'Equip program, Grant 316030_133802/1).

Furthermore, we would like to thank Mrs. Christine Müller-Thompson for the support with editing and typesetting of this manuscript.

Appendix A. Supplementary data

Supplementary data associated with this article can be found, in the online version, at http://dx.doi.org/10.1016/j.aanat.2015.02.007.

References

Aglietti, P., Insall, J.N., et al., 1975. A new patella prosthesis: design and application. Clin. Orthop. Relat. Res. 107, 175–187.
Amis, A., Farahmand, F., 1996. Extensor mechanism of the knee. Curr. Orthop. 10 (2), 102–109.
Borotikar, B., Sheehan, F., 2013. *In vivo* patellofemoral contact mechanics during active extension using a novel dynamic MRI-based methodology. Osteoarthritis Cartilage 21 (12), 1886–1894.
Bourgery, J.-B.-M., 1854. Traité complet de l'anatomie de l'homme comprenant la médecine opératoire.
Carter, D.R., 1984. Mechanical loading histories and cortical bone remodeling. Calcif. Tissue Int. 36 (1), S19–S24.
Carter, D.R., Beaupré, G.S., et al., 2007. Skeletal Function and form: Mechanobiology of Skeletal Development, Aging, and Regeneration. Cambridge University Press, Cambridge.
Eckstein, F., Milz, S., et al., 1998. Thickness of the subchondral mineralised tissue zone (SMZ) in normal male and female and pathological human patellae. J. Anat. 192 (Pt 1), 81–90.
Eckstein, F., Muller-Gerbl, M., et al., 1992. Distribution of subchondral bone density and cartilage thickness in the human patella. J. Anat. 180 (Pt 3), 425–433.
Engelke, K., Karolczak, M., et al., 1999. Micro-CT. Technology and application for assessing bone structure. Der Radiologe 39 (3), 203–212.
Feldkamp, L., Davis, L., et al., 1984. Practical cone-beam algorithm. JOSA A 1 (6), 612–619.
Fitzpatrick, C.K., Baldwin, M.A., et al., 2011. Comparison of patellar bone strain in the natural and implanted knee during simulated deep flexion. J. Orthop. Res. 29 (2), 232–239.
Fox, A.J., Wanivenhaus, F., et al., 2012. The basic science of the patella: structure, composition, and function. J. Knee Surg. 25 (02), 127–142.
Goodfellow, J., Hungerford, D., et al., 1976. Patello-femoral joint mechanics and pathology. 1. Functional anatomy of the patello-femoral joint. J. Bone Joint Surg. (British Volume) 58 (3), 287–290.
Hefzy, M., Jackson, W., et al., 1992. Effects of tibial rotations on patellar tracking and patello-femoral contact areas. J. Biomed. Eng. 14 (4), 329–343.
Hefzy, M., Yang, H., 1993. A three-dimensional anatomical model of the human patello-femoral joint, for the determination of patello-femoral motions and contact characteristics. J. Biomed. Eng. 15 (4), 289–302.
Hehne, H.-J., 1990. Biomechanics of the patellofemoral joint and its clinical relevance. Clin. Orthop. Relat. Res. 258, 73–85.
Hildebrand, T., Laib, A., et al., 1999. Direct three-dimensional morphometric analysis of human cancellous bone: microstructural data from spine, femur, iliac crest, and calcaneus. J. Bone Miner. Res. 14 (7), 1167–1174 (The Official Journal of the American Society for Bone and Mineral Research).
Hildebrand, T., Ruegsegger, P., 1997. Quantification of bone microarchitecture with the structure model index. Comput. Methods Biomech. Biomed. Eng. 1 (1), 15–23.
Hoechel, S., Wirz, D., et al., 2012. Density and strength distribution in the human subchondral bone plate of the patella. Int. Orthop. 36 (9), 1827–1834.
Humphry, G.M., 1858. A Treatise on the Human Skeleton. Macmillan, New York.
Jacobs, C., Yellowley, C., et al., 1998. Differential effect of steady versus oscillating flow on bone cells. J. Biomech. 31 (11), 969–976.
Lanyon, L., Skerry, T., 2001. Perspective: postmenopausal osteoporosis as a failure of bone's adaptation to functional loading: a hypothesis. J. Bone Miner. Res. 16 (11), 1937–1947.
Milz, S., Eckstein, F., et al., 1995. The thickness of the subchondral plate and its correlation with the thickness of the uncalcified articular cartilage in the human patella. Anat. Embryol. (Berl.) 192 (5), 437–444.
Muller-Gerbl, M., 1998. The subchondral bone plate. Adv. Anat. Embryol. Cell Biol. 141 (III–XI), 1–134.
Muller-Gerbl, M., Putz, R., et al., 1989. Computed tomography-osteoabsorptiometry for assessing the density distribution of subchondral bone as a measure of long-term mechanical adaptation in individual joints. Skeletal Radiol. 18 (7), 507–512.
Muller-Gerbl, M., Putz, R., et al., 1990. Demonstration of subchondral density pattern using CT-osteoabsorptiometry (CT-OAM) for the assessment of individual joint stress in live patients. Zeitschrift fur Orthopadie und ihre Grenzgebiete 128 (2), 128–133.
Parfitt, A.M., Drezner, M.K., et al., 1987. Bone histomorphometry: standardization of nomenclature, symbols, and units: report of the ASBMR Histomorphometry Nomenclature Committee. J. Bone Miner. Res. 2 (6), 595–610.
Raux, P., Townsend, P.R., et al., 1975a. Trabecular architecture of the human patella. J. Biomech. 8 (1), 1–7.
Raux, P., Townsend, P.R., et al., 1975b. Trabecular architecture of the human patella. J. Biomech. 8 (1), 1–7.
Scuderi, G.R., 1995. The patella. Springer, New York.
Toumi, H., Higashiyama, I., et al., 2006a. Regional variations in human patellar trabecular architecture and the structure of the proximal patellar tendon enthesis. J. Anat. 208 (1), 47–57.
Toumi, H., Higashiyama, I., et al., 2006b. Regional variations in human patellar trabecular architecture and the structure of the proximal patellar tendon enthesis. J. Anat. 208 (1), 47–57.
Toumi, H., Larguech, G., et al., 2012. Regional variations in human patellar trabecular architecture and the structure of the quadriceps enthesis: a cadaveric study. J. Anat. 220 (6), 632–637.
Townsend, P.R., Miegel, R.E., et al., 1976. Structure and function of the human patella: the role of cancellous bone. J. Biomed. Mater. Res. 10 (4), 605–611.
Townsend, P.R., Raux, P., et al., 1975. The distribution and anisotropy of the stiffness of cancellous bone in the human patella. J. Biomech. 8 (6), 363–367.
Van den Berg, W., 2011. Osteoarthritis year 2010 in review: pathomechanisms. Osteoarthritis Cartilage 19 (4), 338–341.
Wang, L., Ciani, C., et al., 2004. Delineating bone's interstitial fluid pathway in vivo. Bone 34 (3), 499–509.
Wolff, J., 1892. Das Gesetz der Transformation der Knochen. Hirschwald, Berlin.

4.3 Osteoarthritis alters the patellar bones subchondral trabecular architecture

Sebastian Hoechel (1), Hans Deyhle (2), Mireille Toranelli (1), Magdalena Müller-Gerbl (1)

(1) Department of Biomedicine, Musculosceletal Research, University of Basel, Pestalozzistrasse 20, 4056 Basel, Switzerland
(2) Biomaterials Science Center, University of Basel, Gewerbestrasse 14, 4123 Allschwil, Switzerland*

**Supported by the Swiss National Science Foundation (Grant 316030_133802/1)*

Under current revision at the "Journal of Orthopaedic Research"

Motivation:

In case of a faulty relationship between the loading of a joint and the ability of its components to support this biomechanical alteration, the pathogenesis of osteoarthritis (OA) as a disease of the whole joint may arise [41, 42]. Whether the primary lesion, which initiates this process, is located within the cartilage of the joint or the SBP is to date still debated. Nevertheless, models of induced arthritis led to subchondral bone changes where subsequent trabecular remodelling led to a less compliant architectural arrangement followed by excessive stress peaks in the overlying structures [43, 44]. As response, the cartilage reacts with a matrix remodelling and cell proliferation, which significantly alters the pressure transfer onto the SBP.

According to the idea of a functional adaptation, these changes in pressure distribution must have consequences concerning the mineralization of the SBP and the trabecular architecture. Previous studies already began to analyse the effect of OA onto the trabecular network. Authors describe the resulting impairments in OA with an increase in bone volume due to an uncoupled balance between resorption and formation, whether through an increase in trabecular number and a reduced spacing or a simple thickening of trabeculae [45-47].

- ***Aim 3:*** *Taking the above described studies as a base, we aimed to describe the mineralization and the thickness of the SBP of pathologically altered human patellae (Outerbridge classification: grade IV) as marker of the altered long-term load intake of the patella and search for possible alterations within the trabecular architecture in comparison to results of the healthy sample collection of 2.2. Furthermore, the trabecular network was analysed in 1 mm steps (layers), starting just beneath the SBP to a depth of 5 millimetres, in order to describe possible changes in their development as a function of depth.*

Hypothesis:

- Due to cartilage lesion the energy dissipation and spreading within the joint is disrupted – the protection of the underlying SBP is defective and the absolute values of density will be higher with a smaller area of distribution;
- The trabecular network will be larger in volume and surface in order to deal with the higher and less diverted impact forces compared to non-OA samples; and
- The SMI will highly differ in both study groups due to newly developed cross-linked trabecular".

Outcome:

The OA study population, in contrast to the physiological non-OA samples, revealed no specific distribution of maxima as well as minima but presented an irregular distribution pattern in regards to the long-term load intake. Multi-sided maxima and minima of BV/TV, Tb.Th. and Tb.N as well as Tb.Sp. and SMI were present, which did not reveal any regularity.

The trabecular parameters differed significantly in between both sample populations. BV/TV, Tb.Th. and Tb.N showed lower absolute values in the OA group. The difference in relation to the non-OA patella decreased with depth. BV/TV's difference in the 5^{th} mm was 55.8% of that of the first mm, Tb.Th. 77.8% and Tb.N 63.1%. Tb.Sp. and SMI revealed significant higher values, which also decreased in difference to the non-Oa group with depth (Tb.Sp. 51.7%, SMI 46.9%).

Osteoarthritis Alters the Patellar Bones Subchondral Trabecular Architecture

Sebastian Hoechel,[1] Hans Deyhle,[2] Mireille Toranelli,[1] Magdalena Müller-Gerbl[1]

[1]Department of Biomedicine, Musculoskeletal Research, University of Basel, Pestalozzistrasse 20, 4056 Basel, Switzerland, [2]Biomaterials Science Center, University of Basel, Gewerbestrasse 14, 4123 Allschwil, Switzerland

Received 25 November 2015; accepted 11 November 2016
Published online in Wiley Online Library (wileyonlinelibrary.com). DOI 10.1002/jor.23490

ABSTRACT: Following the principles of "morphology reveals biomechanics," the cartilage-osseous interface and the trabecular network show defined adaptation in response to physiological loading. In the case of a compromised relationship, the ability to support the load diminishes and the onset of osteoarthritis (OA) may arise. To describe and quantify the changes within the subchondral bone plate (SBP) and trabecular architecture, 10 human OA patellae were investigated by CT and micro-CT. The results are presented in comparison to a previously published dataset of 10 non-OA patellae which were evaluated in the same manner. The analyzed OA samples showed no distinctive mineralization pattern in regards to the physiological biomechanics, but a highly irregular disseminated distribution. In addition, no regularity in bone distribution and architecture across the trabecular network was found. We observed a decrease of material as the bone volume and trabecular thickness/number were significantly reduced. In comparison to non-OA samples, greatest differences for all parameters were found within the first mm of trabecular bone. The differences decreased toward the fifth mm in a logarithmic manner. The interpretation of the logarithmic relation leads to the conclusion that the main impact of OA on bony structures is located beneath the SBP and lessens with depth. In addition to the clear difference in material with approximately 12% less bone volume in the first mm in OA patellae, the architectural arrangement is more rod-like and isotropic, accounting for an architectural decrease in stability and support. © 2016 Orthopaedic Research Society. Published by Wiley Periodicals, Inc. J Orthop Res

Keywords: osteoarthritic trabecular changes; human patella; subchondral bone plate mineralization; 3D micro-CT

Bone, as dynamic tissue, constantly balances its formation and resorption process to maintain an optimal supportive structure and meet the mechanical demands. In accordance to the biomechanics of a joint and the resulting pressure distribution, these adaptational processes can be seen in the distribution pattern of the thickness and mineral distribution of the subchondral bone plate (SBP).[1–7] Following these principles of "morphology reveals biomechanics," the mineral distribution of the SBP and the architecture of the trabecular just beneath show similar morphologic characteristics. Maxima of mineral embedment are regularly found in the more heavily loaded areas within the SBP of a joint surface. Therefore, such maxima are found on the talar edges, decreasing toward the center of the medial groove,[8] on the medial condyle of the tibial plateau in comparison to the lateral,[3] and on the lateral patellar facet.[9] The latter one is due to the greater contact force applied to the lateral facet through the displacement vector of the quadriceps muscle (quadriceps angle).

The dynamics of these density patterns in regards to changes of the biomechanics following pathological conditions were shown in an animal meniscectomy model where the maxima of mineralization shifted following the altered mechanical situation.[10] Studies on patients following tibial osteotomy for genu varum also revealed a shift of maxima location after successful realignment. One year postoperative, peak mineralization on the medial condyle centralized, and the lateral condyle showed increased calcium hydroxyapatite deposition, corresponding to the theoretical expectations.[6] Since the SBP links to the cancellous bone beneath, the absorbed load is forwarded into the trabecular system. Here, the trabecular bone adapts to the mechanical environment as a function of the pressure which is put forward.[11] Following the applied theorems of stereology on 2D sections of early investigations, direct three-dimensional (3D) measurements have emerged. Now it is possible to determine the microarchitecture of trabecular bone in a direct manner, saving the time consuming sectioning process and the inaccuracy of assumptions.[12–14] In addition to the common differences in trabecular architecture as function of anatomic position, loading direction, and load accumulation over time,[15,16] precise correlations to individual long-term load intake are described.[17,18]

In case of a compromised relationship between the loading in a joint and the ability of its components to support the load, the pathogenesis of osteoarthritis (OA) as a disease of the whole joint may arise.[19–21] Next to typical cartilage lesions, changes within the subchondral bone seem to play an important role in the dynamics of the disease. Whether the cartilage lesions are the trigger factor or a secondary consequence of the subchondral bone changes is still debated.[22] Nevertheless, models of induced OA lead to subchondral bone changes with subsequent trabecular remodeling resulting in a less compliant trabecular bone, and therefore, excessive stress in the overlying articular cartilage.[23,24]

Conflicts of interest: None.
Grant sponsor: Swiss National Science Foundation; Grant number: 316030_133802/1.
Correspondence to: Sebastian Hoechel, (T: +41 (0) 61 267 39 37; F: +41 (0) 61 267 39 59; E-mail: sebastian.hoechel@unibas.ch)

As one of the most severe causes of knee pain in the elderly population, patellofemoral OA changes lead to anterior knee pain causing difficulties in daily routine including gait, stairs, and squatting.[25,26] The resulting impairments of function as well as the pain are thought to be the consequence of trauma or changes within the pressure distribution of the patellofemoral joint particularly following meniscal tear or rupture of the cruciate ligaments.[27,28]

As for the patella, the literature describes cartilage lesions more severe than Outerbridge Grade II in more than 63% in the elderly population. Here, the depth of the lesion correlates to the anterior knee pain. Also, it has been shown that females are more affected by cartilage lesions than males.[29]

The architectural changes within the subchondral bone of the patella can until now only be assumed using the existing concepts of OA, where non-physiological strain initiates a cascade reaction of bone alteration.

In this case, the early onset of cartilage degeneration is accompanied by a sclerosis of the SBP and an increase in trabecular thickness and density. It leads to a progressive change of trabeculae form rodlike to platelike, the opposite of the processes in normal aging.[30] Late-stage OA (according to the Kellgren and Lawrence radiographic criteria: grade 4) on the other hand, shows a decrease of bone mineral density.[31]

To further evaluate this effect of late stage OA and describe the changes occurring in the trabecular architecture, this study analyses directly derived 3D-micro-CT data models, to gain information of architectural trabecular parameters as a function of localization.

We therefore, aim to describe the regional distribution of bone parameters and their correlation to the individual long-term load intake via:

(1) The description of the mineralization and the thickness of the SBP in late-stage OA patellae as markers of the long-term load intake;
(2) The evaluation of the trabecular architecture of late-stage OA patellae
    a. Beneath the entire SBP to achieve demonstration of the regional distribution
    b. In 1 mm steps (layers), starting just beneath the SBP to a depth of 5 mm to describe the development of OA into depth.

Since the anatomy of the SBP and trabecular network of 10 non-OA patellae of the elderly population has already been described we intent to:

(3) Compare the findings to a previously published dataset of non-OA samples which were in the same age group and analyzed using the same methods to directly draw conclusions on the late-stage OA changes of the trabecular network.

MATERIALS AND METHODS

Materials

Ten formalin-fixed, OA human patellae were used (five male, five female; age 60–74 years, mean 69.4; unknown medical history). The inclusion criteria was specified as cartilage degeneration of Outerbridge IV on the medial and/or lateral facets.

In consideration of The Code of Ethics of the World Medical Association (Declaration of Helsinki), for experiments involving humans, the samples were taken from body-donors to the Department of Anatomy, University of Basel, who contributed their body to science and research only.

Methods

Density Distribution of the Subchondral Bone Plate

Using conventional CT-datasets (SOMATOM 16, Siemens, Erlangen, Germany, 120 kilovolt [kV], 180 milliampere-second [mAs], slice thickness 0.6 mm, axial slices) of the samples, we evaluated the density distribution of the SBP with the help of the software ANALYZE® 11.0 (Biomedical Imaging Resource, Mayo Foundation, Rochester, MN). According to the mineral content, the "maximum intensity projection-algorithm" projects the densest voxel within the SBP onto the surface in a color-coded manner. Starting with Hounsfield units (HU) greater than 1,200 in black, the colors descended in steps of 200 HU to red, yellow, green, and blue.[6,17,32]

The CT-osteoabsorptiometry method has been evaluated using dual-energy quantitative computed tomography and validated in comparison to the analysis of fresh and frozen samples (discrepancy of 0.5%).[6] Therefore, the density distribution with respect to the HU directly links to the calcium hydroxyapatite concentration, which was calculated.

Micro-CT Measurements

Micro-CT experiments were performed with the General Electric phoenix nanotom® m system (Wunstorf, Germany) with an acceleration voltage of 140 kV, beam current of 60 μA, and a 0.1 mm aluminum-filter to reduce beam-hardening. The patella was placed in a polyethylene container filled with fixation solution to prevent the tissue from drying. The 2,100 projections (exposure time: 0.5 s) were recorded over 360 degrees, defining the resulting isotropic pixel size of 32 μm. Reconstruction was performed with the datosx software (GE, Wunsdorf, Germany) based on a modified Feldkamp algorithm.[33]

In accordance to a previously conducted study on non-OA patellae, the 3D datasets of the patellae were divided into 21 measuring cubes ($8 \times 8\,mm^2 \times$ SBP to anterior cortical bone) using the visualization and analysis software VGStudio® Max 2.2 (Heidelberg, Germany).[17] All cubes were separately analyzed to present a topographical parameter distribution across the entire articulation surface.

In the first step, the thickness of the SBP was evaluated. Following this evaluation, the trabecular bone of the first 5 mm (1st ROI: 0–1 mm of trabecular bone below the SBP, 2nd ROI: 1–2 mm, likewise for the 3rd, 4th, and 5th ROI) beneath the SBP of the produced measuring cubes were analyzed (Fig. 1) with the help of the Skyscan software CT-analyser® (Bruker-Microct, Kontich, Belgium).[17] All analysis were performed using an automatic surface detection system in accordance to the threshold distribution of the dataset and provide a complete inter-observer independence.

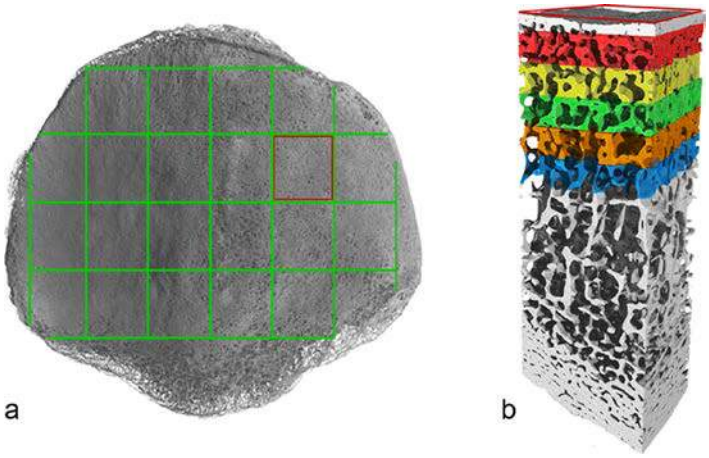

Figure 1. Method of μ-CT; definition of measurement cube and regions of interest. a) 3D reconstruction, left patella in dorsal view, 21 areas for extraction of measurement cubes marked. b) Measurement cube with five highlighted regions of interest (1st ROI: red; 2nd ROI: yellow; 3rd ROI: green; 4th ROI: orange; 5th ROI: blue) just below the subchondral bone plate.

The obtained parameters of bone histomorphometry and architecture were selected according to literature recommendations of bone analysis and are as follows[13,34–36]:

(1) BV/TV, (%); indices of bone volume (BV) in relation to the total volume (TV); a parameter of trabecular bone that is contained within a biphasic region of solid structure and space, it resembles the proportion of the ROI occupied by solid material;
(2) BS/TV, (1/mm); bone surface density (BS) in relation to the TV; this 3D trabecular surface is based on the faceted surface of the binarised ROIs and describes the bone surface per TV in every 1 mm ROI across the whole patellar articular surface;
(3) Tb.Th, (mm); parameter of dimension for the trabecular thickness; truly measured, model-independent parameter that determines an average of the local thickness at each voxel representing bone. It is defined as diameter of a sphere, which encloses the point (not necessarily the center) and is still entirely contained within the solid surfaces; and
(4) Tb.Sp, (mm); trabecular separation; directly and model-independently measured in 3D by the same method used to measure trabecular thickness; as primary measurements in bone histomorphometry.

Derived indices:

(5) Tb.N, (1/mm); the trabecular number; it implies the number of traversals across a trabecular made per unit length on a linear path through a bony region and is measured in 3D by application of an equation for the parallel plate model using direct 3D measurements of Tb.Th and BV/TV; as structural parameter. As well as:
(6) SMI, (dimensionless); the structure model index; indicating the relative prevalence of plate-like or rod-like architecture within the 3D trabecular network. It involves a measurement of the surface convexity and is based on dilation of the 3D voxel model, which is the artificial addition of one voxel thickness to all binarised object surfaces. The SMI values of an ideal plate, cylinder, and sphere model are 0, 3, and 4, respectively; and
(7) DA, (dimensionless); the degree of anisotropy; describing the presence or absence of the alignment of structures preferentially along a particular directional axis. Results of DA range from 0 (total isotropy) to 1 for total anisotropy, that can be described as columns of trabecular without interconnections.

Statistical Analysis

Depth based data analyses were performed for every measuring cube. Afterward, the mean value of all ROIs on the same level for every analyzed parameter was used as result.

The presented data were analyzed for each patella. The results are referenced to the data collected on a non-OA sample population (five male and five female; mean age 72 years, range 65–78 years; six right samples, four left) from a previous study, where the same methods and analysis techniques were used.[17]

Statistical analysis included the Pearson product-moment correlation coefficient, a two-tailed *t*-test stating the significance as well as the Kolmogorov–Smirnov test for evaluation of the distribution level of the data. A p-value of <0.05 was considered as statistically significant. All analyses were performed using RStudio® (RStudio®: Integrated-development environment for R, Version 0.99.467, Boston, MA).

RESULTS

Mineral Distribution of the Subchondral Bone Plate

The mineralization within the SBP of the OA population showed a strong irregularity with multi-located spot like maxima covering the whole articulating surface. Especially in areas where completely detached chondral fragments were present, these maxima were often surrounded by lacunae of low mineralization with differences of up to 400–450 mg/ml. Furthermore, the pathological osteophyte formations around the rim showed a high variation of calcium hydroxyapatite with local peaks of enrichment (Fig. 2b).

In comparison to the non-OA population (Fig. 2a), there were no signs of regularity for the pattern of mineral distribution. The positions of the found maxima and minima were in no relation to a physiological load distribution within the patellofemoral joint. The absolute range of mineralization of the evaluated maxima and minima did not differ significantly

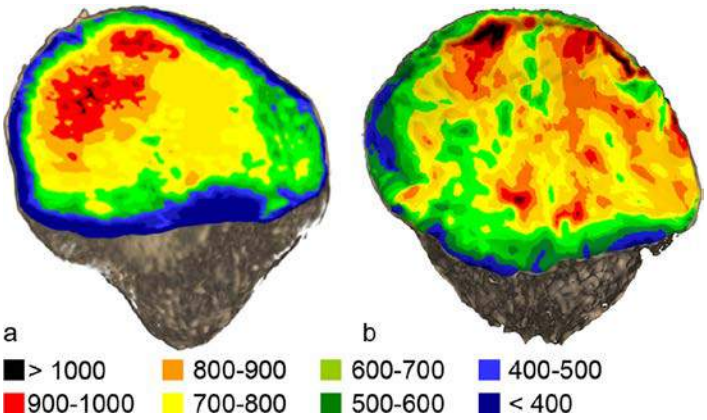

Figure 2. Representative mineralization pattern according to the density distribution of the human patella (mg/ml calcium hydroxyapatite; left = lateral). a) Non-OA patella[17] b) OA patella.

($p = 0.43$) in comparison to the non-OA samples. The peak values of the maxima ranged from 845 to 1,080 mg/ml (non-OA samples: 880–1,047 mg/ml), the lowest measured mineral values ranged from 380 to 420 mg/ml (non-OA samples: 377–437 mg/ml) (Fig. 2a and b).

Micro-CT Measurements

Subchondral Bone Plate Thickness

The SBP of OA patellae presented itself as solid, homogenous build but contained wave-like lamella with a BV/TV of 96–98% (standard deviation (SD) 1.6). Its thickness distribution revealed two maxima with one obvious minimum in between. The maxima were located on the lateral facet (up to 1.25 mm; mean 1.11 mm; SD 0.20 mm) as well as on the medial facet (up to 1.05 mm; mean 0.84 mm; SD 0.25 mm). The minimum of the subchondral bone thickness was situated on the vertical ridge of the patellae, presenting a mean thickness of 0.65 mm (SD 0.35 mm) in its distal parts. The difference between maximum and minimum was statistically significant ($p < 0.05$) (Fig. 3b).

In contrast to the SBP thickness of the OA samples, the non-OA sample population showed only one maximum located on the lateral facet (up to 1.25 mm; mean 1.16 mm; SD 0.25 mm), which gradually decreased toward the periphery including one medial extension with a thickness of 0.65–0.80 mm over the vertical ridge onto the medial facet.

While the SBP of the non-OA samples showed a smooth border in its transition to the calcified cartilage, the OA samples showed a more wave-like appearance extending into an osteophyte formation at its borders to the anterior cortical bone. Comparing the SBP-thickness of both sample collections, no significant difference ($p > 0.05$) was found (Fig. 3a and b).

Trabecular Measurements

The OA population revealed no noticeable distribution pattern of the obtained trabecular measurements within the first 5 mm of analyzed spongy bone. Multiside maxima and minima of all analyzed parameters were present. Still, BV/TV, BS/TV, Tb.Th, and Tb.N showed a steady decrease of absolute value into depth, where the decrease of the absolute parameter value per mm of depth declined with depth showing the largest differences between the first and second mm. This was a steady but declining decrease, and therefore, the development of each of the parameters into

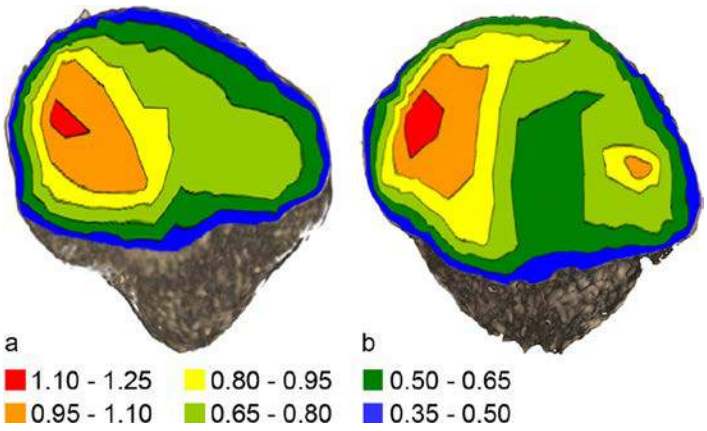

Figure 3. Summation chart of the thickness distribution of the subchondral bone plate (mm; left = lateral). a) Non-OA patellae[17] b) OA patellae.

depth could be described as a logarithmic dependency (Fig. 4). For Tb.Sp, SMI, and DA, an ongoing increase was seen. For these observations, the increase was highest between the first and the second mm and decreased toward the fourth and fifth mm. The dependency of these parameters from depth showed a logarithmic dependency (Fig. 4).

In comparison to the non-OA group, BV/TV, BS/TV, Tb.Th., and Tb.N showed significantly ($p < 0.05$) lower values in the OA group in every analyzed depth in comparison to the non-OA sample collection (Fig. 4). The differences of the absolute value between each layer decreased with depth in the sample, showing the largest absolute differences in the 1st mm, the smallest differences in the 5th mm respect to the absolute value of the non-OA sample reduced in depth.

On the contrary, Tb.Sp, DA, and SMI revealed significantly ($p < 0.05$) higher values in the OA sample population in comparison to the non-OA population (Fig. 4). Here as well, the difference of the absolute parameter value as well as the calculated difference in comparison to the absolute value of the non-OA sample population decreased with depth and revealed the smallest difference in the 5th mm.

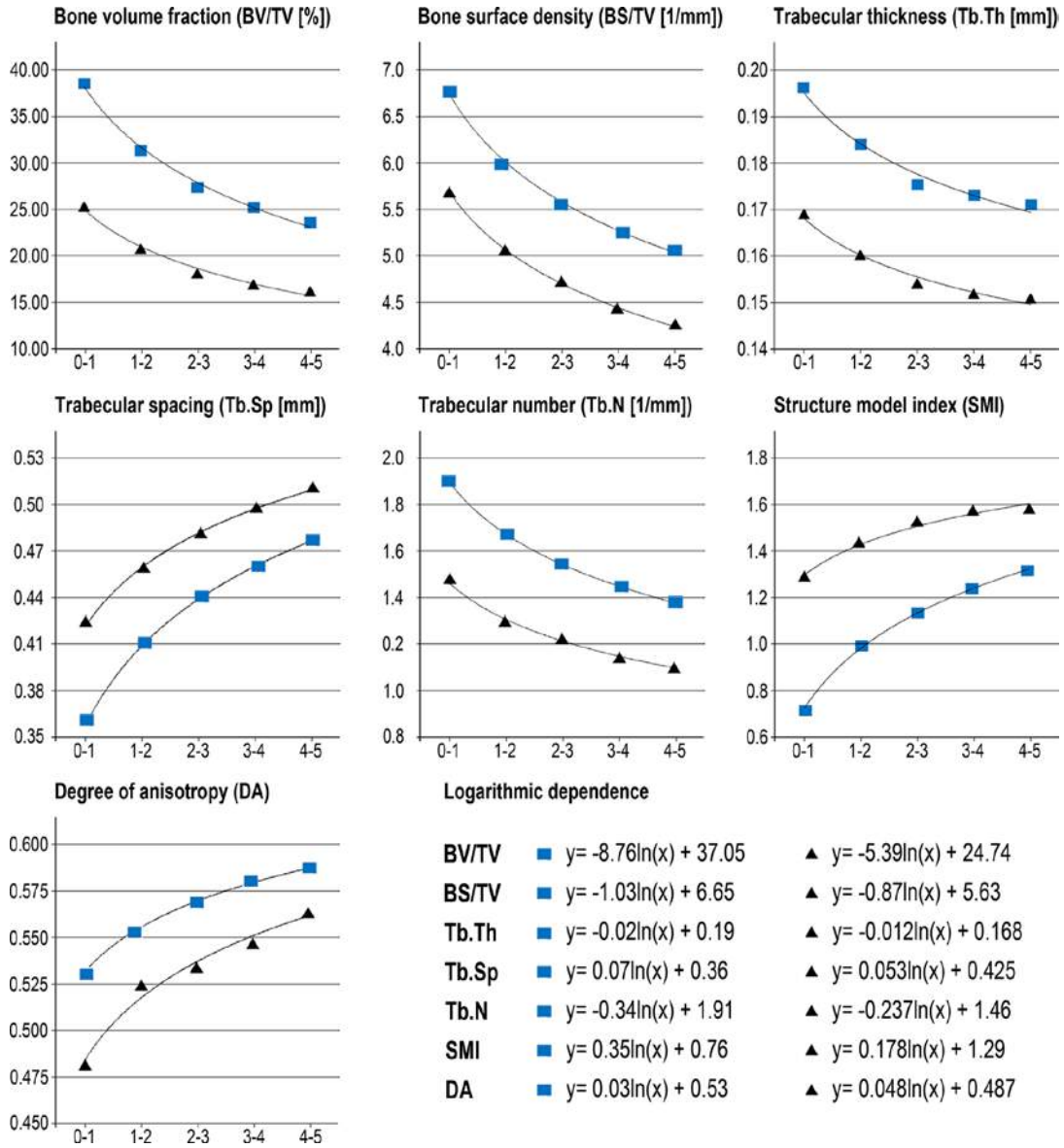

Figure 4. Logarithmic dependency of the architectural parameter development from the first to the fifth millimetre of trabecular bone beneath the subchondral bone plate of the human patella. ■) Non-OA patellae; ▲) OA patellae.

DISCUSSION

In the patella, a chondromalacia or cartilage softening of the lateral facet follows secondary to excessive pressure.[37] On the medial facet, a non-physiological combination of compression and shear stress is described to be the initiating factor.[37] In the end, this loss of elasticity as it is induced by cartilage softening, decreases the functional ability to distribute pressure throughout the articular cartilage, and leads to a mechanical situation where the articular forces are transferred abnormally onto the SBP provoking an adjacent reaction.[37]

Following previous studies of the adaptation of the SBP to pathologically altered long-term load intake, this irregular distribution would result in an abnormal density distribution pattern that can clearly be differentiated from the ones observed in non-OA samples.[9,38,39]

The constant maximum of density and therefore, the deposition of calcium hydroxyapatite on the lateral facet of the patella, as previously described on non-OA samples, was not observed in this study.[6,38] Instead, the deposition was spot-like scattered over the entire joint surface, revealing a long-term load intake that is not in correlation to the applied pressure. In between the spots of high density, lacunae of very low concentration were present.

The mean SBP's thickness distribution over all OA samples represented two maxima, one on the medial and one on the lateral facet. Located on the ridge, we observed a significant minimum. The often-described sclerosis and thickening of the SBP in OA patients can be attributed to the spot-like deposition of calcium hydroxyapatite forming the second maximum on the medial facet as it is not seen in a non-OA study group.[40,41] There, the SBP presented itself significantly ($p < 0.5$) thicker. A significant increase or decrease of the total thickness was not observed. These results do not implicate a more severe change within the medial facet, but a non-physiologic mineralization throughout the SBP of the patella which only than raises the mineralization of the medial side. Nevertheless, on the lateral facet, where the mineral content is higher in general, the now irregular distribution is on the same level as a non-OA hydroxyapatite concentration.

These results are in agreement to previously published data from Eckstein et al. who showed that cartilage lesions lead to a thickening of the SBP in the affected area without exceeding the maximum thickness of non-OA samples.[9] Previously described advancing endochondral ossification and multiplication of the tidemark as well as new bone formation was not seen in this study.[42,43] A partial explanation might be the production of new, un-mineralized, and immature bone formation without the equivalent mineralization, leading to thicker, but less resistant bone that would not be visible during this micro CT analysis.[44]

Since the changes within the cartilage-osseous interface led to alterations of pressure (distribution and) transfer into the trabecular bone system, differences in the 3D network, compared to the non-pathological situation, demonstrate the expected bone turnover associated with OA.

In contrast to studies using bone-cores or cuts from selected areas of OA degenerated bones, we acquired data for the whole trabecular network of pathological patellae for comparison with a non-OA sample collection. Our data allows accessing the trabecular architecture of entire patellae 5 mm in depth under the SBP and is not limited to selected measurements resembling the architectural situation.[45] A comparison of absolute values with those from literature is therefore, difficult, and parallels should only be drawn concerning the statements about the differences of non-OA and OA.

In general, we observed a decrease of material in the OA population, as the BV as well as the trabecular number and thickness decreased, and the trabecular spacing was significantly wider ($p < 0.1$). These results are in agreement with the study by Dedrick et al., who showed a reduced Tb.Th in severe OA, as well as with Ding et al. who also demonstrated a decrease in trabecular bone structure and mechanical properties in OA.[46,47] Recently published results of an anterior cruciate ligament transection model in a rabbit also demonstrated significant reduction of BV/TV and Tb.Th in the medial femoral compartment of the OA knee.[48]

In contrast, analyses of the femorotibial joint published by Kamibayashi et al. and Buckland-Wright et al. showed an increase of BV/TV, due to thick, widely spaced trabecular.[49,50] In regards to the measurement acquisition, one has to note that Kamibayashi et al. used stained histologic sample analysis of 2D images only on the medial tibial plateau and Buckland-Wright et al. used conventional X-ray summation images, which projects the 3D arrangement on a 2D picture, lacking in representation value, and the direct description of the third dimension. Although these methods give insight into the OA of the femorotibial joint, micro CT measurements allow accessing the 3D structure.

Overall, this study substantiates and expands upon the results of Patel et al. published in 2003.[45] They analyzed bone-core specimens from normal and OA knees and described the differences of trabecular parameters for the medial tibial plateau, where they found the most significant differences. They described the BV/TV and Tb.Th to be lower in the OA samples with SMI and Tb.Th being higher, in agreement with our results. Tb.N showed no significant variation, whereas in the patella we observed a significant reduction in the OA sample collection.

Examining the development of the architectural parameters into the depth of the trabecular network we found a logarithmic dependency that showed the greatest difference for all parameters within the first mm, decreasing toward the fifth. This led us to the conclusion that the main impact of OA is beneath the

SBP and lessens with depth. Next to the clear distinction in the amount of material with approximately 12% less BV in the first mm, the architectural arrangement shows a more rod-like and isotropic arrangement just beneath the SBP in OA in comparison to the plate-like and more anisotropic physiological arrangement. As stated above, the absolute differences decrease with depth and the logarithmic dependencies of the non-OA and OA samples show a narrowing of the curves toward the 5th mm. We cannot exclude a gain of material in initial stages of OA. In the advanced cases observed here, BV loss was always observed, and was most severe just below the mechanically altered SBP and is mostly due to a consequence of a reduced trabecular number (−23.20% in the first mm) than to the reduction of the trabecular thickness (−13.29% in the first mm).

The limitations of this study must be seen in the lack of knowledge of the medical-history of the body-donors concerning knee injuries as well as the limited number of samples. Furthermore we did not differentiate between male and female patellae. Merely the OA stage according to Outerbridge was of importance for sample collection. Although we compared OA patellae with non-OA patellae from a previous study, the methods used were exactly the same.

In conclusion, the data points to a decrease of OA activity with depth beneath the SBP and underlines the idea that the development of the disease starts well above the SBP and trabecular network and progress downwards. Future studies on cell level will have to determine the reasons of differences in bone turnover in the consecutive mms within the trabecular system and aim to explain the cell-mechanisms behind.

AUTHORS' CONTRIBUTIONS

Sebastian Hoechel and Magdalena Müller-Gerbl designed the study. Sebastian Hoechel and Mireille Toranelli contributed to analysis and interpretation. Hans Deyhle committed to data acquisition and processing. Sebastian Hoechel drafted and finalized the paper. All authors have read and approved of the final manuscript.

REFERENCES

1. Simkin PA, Graney DO, Fiechtner JJ. 1980. Roman arches, human joints, and disease. Arthritis Rheum 23:1308–1311.
2. Simkin PA, Heston TF, Downey DJ, et al. 1991. Subchondral architecture in bones of the canine shoulder. J Anat 175:213.
3. Clark JM, Huber JD. 1990. The structure of the human subchondral plate. J Bone Joint Surg Br 72:866–873.
4. Milz S, Eckstein F, Putz R. 1997. Thickness distribution of the subchondral mineralization zone of the trochlear notch and its correlation with the cartilage thickness: an expression of functional adaptation to mechanical stress acting on the humeroulnar joint? Anat Rec 248:189–197.
5. Milz S, Putz R. 1994. Quantitative morphology of the subchondral plate of the tibial plateau. J Anat 185:103–110.
6. Muller-Gerbl M. 1998. The subchondral bone plate. Adv Anat Embryol Cell Biol 141:1–134.
7. Zumstein V, Kraljević M, Müller-Gerbl M. 2013. Glenohumeral relationships: subchondral mineralization patterns, thickness of cartilage, and radii of curvature. J Orthop Res 31:1704–1707.
8. Leumann A, Valderrabano V, Hoechel S, et al. 2015. Mineral density and penetration strength of the subchondral bone plate of the talar dome: high correlation and specific distribution patterns. J Foot Ankle Surg 54:17–22.
9. Eckstein F, Muller-Gerbl M, Putz R. 1992. Distribution of subchondral bone density and cartilage thickness in the human patella. J Anat 180:425–433.
10. Anetzberger H, Mayer A, Glaser C, et al. 2014. Meniscectomy leads to early changes in the mineralization distribution of subchondral bone plate. Knee Surg Sports Traumatol Arthrosc 22:112–119.
11. Wolff J. 1986. The law of bone remodeling [translated from the 1892 original, Das Gesetz der Transformation der Knochen, by P. Maquet and R. Furlong]. Berlin: Springer Verlag.
12. Ding M, Odgaard A, Hvid I. 1999. Accuracy of cancellous bone volume fraction measured by micro-CT scanning. J Biomech 32:323–326.
13. Hildebrand T, Laib A, Müller R, et al. 1999. Direct three-dimensional morphometric analysis of human cancellous bone: microstructural data from spine, femur, iliac crest, and calcaneus. J Bone Miner Res 14:1167–1174.
14. Hildebrand T, Rüegsegger P. 1997. A new method for the model-independent assessment of thickness in three-dimensional images. J Microsc 185:67–75.
15. Evans FG, King AI. 1961. Regional differences in some physical properties of human spongy bone. Biomechanical studies of the musculo-skeletal system. IL: Charles C Thomas Springfield. p 19–67.
16. Goldstein SA. 1987. The mechanical properties of trabecular bone: dependence on anatomic location and function. J Biomech 20:1055–1061.
17. Hoechel S, Schulz G, Müller-Gerbl M. 2015. Insight into the 3D-trabecular architecture of the human patella. Ann Anat 200:98–104.
18. Nowakowski AM, Deyhle H, Zander S, et al. 2013. Micro CT analysis of the subarticular bone structure in the area of the talar trochlea. Surg Radiol Anat 35: 283–293.
19. Sun HB. 2010. Mechanical loading, cartilage degradation, and arthritis. Ann NY Acad Sci 1211:37–50.
20. Valderrabano V, Horisberger M, Russell I, et al. 2009. Etiology of ankle osteoarthritis. Clin Orthop Relat Res 467:1800–1806.
21. Tecklenburg K, Dejour D, Hoser C, et al. 2006. Bony and cartilaginous anatomy of the patellofemoral joint. Knee Surg Sports Traumatol Arthrosc 14:235–240.
22. Madry H, van Dijk CN, Mueller-Gerbl M. 2010. The basic science of the subchondral bone. Knee Surg Sports Traumatol Arthrosc 18:419–433.
23. Radin EL, Parker HG, Pugh JW, et al. 1973. Response of joints to impact loading—III: relationship between trabecular microfractures and cartilage degeneration. J Biomech 6:51–57.
24. Burr DB, Martin RB, Schaffler MB, et al. 1985. Bone remodeling in response to in vivo fatigue microdamage. J Biomech 18:189–200.
25. Sharma L, Kapoor D. 2007. Epidemiology of osteoarthritis. Osteoarthritis: diagnosis and medical/surgical management. Philadelphia: PA Saunders. p 3.
26. Guccione AA, Felson DT, Anderson JJ, et al. 1994. The effects of specific medical conditions on the functional limitations of elders in the Framingham study. Am J Public Health 84:351–358.

27. Neuman P, Kostogiannis I, Fridén T, et al. 2009. Patellofemoral osteoarthritis 15 years after anterior cruciate ligament injury—a prospective cohort study. Osteoarthritis Cartilage 17:284–290.
28. Englund M, Lohmander L. 2005. Patellofemoral osteoarthritis coexistent with tibiofemoral osteoarthritis in a meniscectomy population. Ann Rheum Dis 64:1721–1726.
29. Iriuchishima T, Ryu K, Aizawa S, et al. 2012. Evaluation of the prevalence, lesion, and depth of osteoarthritic changes in the patella. Knee Surg Sports Traumatol Arthrosc 20:2460–2464.
30. Ding M. 2010. Microarchitectural adaptations in aging and osteoarthrotic subchondral bone issues. Acta Orthop Suppl 81:1–53.
31. Hannan MT, Anderson JJ, Zhang Y, et al. 1993. Bone mineral density and knee osteoarthritis in elderly men and women. The Framingham study. Arthritis Rheum 36:1671–1680.
32. Muller-Gerbl M, Putz R, Hodapp N, et al. 1989. Computed tomography-osteoabsorptiometry for assessing the density distribution of subchondral bone as a measure of long-term mechanical adaptation in individual joints. Skeletal Radiol 18:507–512.
33. Feldkamp L, Davis L, Kress J. 1984. Practical cone-beam algorithm. JOSA A 1:612–619.
34. Dempster DW, Compston JE, Drezner MK, et al. 2013. Standardized nomenclature, symbols, and units for bone histomorphometry: a 2012 update of the report of the ASBMR Histomorphometry Nomenclature Committee. J Bone Miner Res 28:2–17.
35. Hildebrand T, Ruegsegger P. 1997. Quantification of bone microarchitecture with the structure model index. Comput Methods Biomech Biomed Engin 1:15–23.
36. Parfitt AM, Drezner MK, Glorieux FH, et al. 1987. Bone histomorphometry: standardization of nomenclature, symbols, and units: report of the ASBMR Histomorphometry Nomenclature Committee. J Bone Miner Res 2:595–610.
37. Ficat RP, Hungerford DS. 1977. Disorders of the patellofemoral joint. Baltimore: Williams & Wilkins.
38. Hoechel S, Wirz D, Muller-Gerbl M. 2012. Density and strength distribution in the human subchondral bone plate of the patella. Int Orthop 36:1827–1834.
39. Muller-Gerbl M, Weisser S, Linsenmeier U. 2008. The distribution of mineral density in the cervical vertebral endplates. Eur Spine J 17:432–438.
40. Burr DB, Gallant MA. 2012. Bone remodelling in osteoarthritis. Nat Rev Rheumatol 8:665–673.
41. Henrotin Y, Pesesse L, Sanchez C. 2012. Subchondral bone and osteoarthritis: biological and cellular aspects. Osteoporos Int 23:847–851.
42. Thambyah A, Broom N. 2009. On new bone formation in the pre-osteoarthritic joint. Osteoarthritis Cartilage 17:456–463.
43. Suri S, Walsh DA. 2012. Osteochondral alterations in osteoarthritis. Bone 51:204–211.
44. Lories RJ, Luyten FP. 2011. The bone-cartilage unit in osteoarthritis. Nat Rev Rheumatol 7:43–49.
45. Patel V, Issever AS, Burghardt A, et al. 2003. MicroCT evaluation of normal and osteoarthritic bone structure in human knee specimens. J Orthop Res 21:6–13.
46. Dedrick, D.K., Goldstein SA, Brandt KD, et al., 1993. A longitudinal study of subchondral plate and trabecular bone in cruciate-deficient dogs with osteoarthritis followed up for 54 months.
47. Ding M, Hvid I. 2000. Quantification of age-related changes in the structure model type and trabecular thickness of human tibial cancellous bone. Bone 26:291–295.
48. Florea C, Malo MKH, Rautiainen J, et al. 2015. Alterations in subchondral bone plate, trabecular bone and articular cartilage properties of rabbit femoral condyles at 4 weeks after anterior cruciate ligament transection. Osteoarthritis Cartilage 23:414–422.
49. Kamibayashi L, Wyss UP, Cooke TDV, et al. 1995. Trabecular microstructure in the medial condyle of the proximal tibia of patients with knee osteoarthritis. Bone 17:27–35.
50. Buckland-Wright J, Lynch J, Macfarlane D. 1996. Fractal signature analysis measures cancellous bone organisation in macroradiographs of patients with knee osteoarthritis. Ann Rheum Dis 55:749–755.

5 Summary

The cornerstone of the presented studies is the concept of functional adaptation of the musculoskeletal system. In detail, it is the fact that bone, as rigid as it is, is a dynamic component within the human body that adapts to its mechanical needs over time.
The basis and initial foundation of this concept clearly is the work of Julius Wolff, who, in his 1892 published main work, described the functional adaptation and transformation of bone in accordance to the pressure and stress that is put on it. He, with his main work, established the autonomy of Orthopaedics, which enabled the launch of the “German Orthopaedic Society” (“Deutsche Gesellschaft für Orthopädie”) in 1902.
Following his ideas, many researches as well as critics, worked for decades to increase the knowledge of musculoskeletal adaptation through the difference in load distribution down to the level of genetic predisposition.
The presented thesis deals with the macroscopic and microscopic structural adaptation of the SBP and trabecular architecture of the human patella.
As main tool for analysis, the Method of CT-OAM was used to provide an insight into the long-term loading history of every individual sample. By the visualization of the density distribution, as it is acquired through conventional CT investigations, the mineralization as mirror of the long-term loading history resembles the biomechanical situation of every individual patella. Since in healthy PFJs the main load is transmitted onto the lateral facet of the patella, CT-OAM showed the highest density there.
As functional adaptation of the SBP to the present biomechanical situation, its mechanical properties show significant correlations. Not only is the thickness of the SBP the highest in areas of high density, but also penetration strength as mechanical property proofed to have its peak here.
The trabecular network just below the SBP also revealed structural properties in accordance to the biomechanical situation represented by CT-OAM. Structural parameters which describe an accumulation of bone in order to maximize the support were found to have peak values just beneath areas of high density. These maxima, in correlation with the density, decreased towards the periphery where less support is necessary. Altogether, one can say that the trabecular network, in its way to support the SBP, adapts to its needs by using as much material as necessary and as less as possible. Interestingly, the parameters also showed a more homogenous distribution within the depth of 5 mm than just below the SBP. Following Wolff’s law, this can be

seen as adaptation to the more equally distributed forces within the depth of the bone in comparison to just beneath the articular surface.

Next to the described adaptational bone formation, the last study dealt with the transformation of bone. The evaluated OA samples clearly revealed a long-term distribution within the SBP that was not physiologic. No regularities of density distribution were found. Maxima and minima were spot-like scattered over the entire SBP. Here, the altered density distribution reveals a pathological transformation of the SBP in response to the difference in pressure distribution from the cartilage above. In consequence, the trabecular network below transformed as well. Regularities, as there were found within the healthy population, were not seen. The evaluated parameters showed a highly inhomogeneous distribution but revealed generally less bony material in comparison to the healthy samples. The absolute difference of bone in comparison to the healthy collection reduced with depth, accounting for a decrease of the effect of the OA with depth.

Altogether, the results from the analysis of the human patellae nicely show and describe the structural adaptation of bone to the applied long-term loading history and ones again, follow Wolff’s hypothesis.

6 Conclusions and Outlook

The beautiful and extraordinary designs in mammals and plants have undoubtedly fascinated people throughout history but are perhaps nowhere as evident as in the musculoskeletal system of men.

In muscles, ligaments, tendons, bones and cartilage of all vertebras we see a delicately order that manifests itself as organ, tissue and cells down to the molecular level. This hierarchy is not random, but exists as a harmony of complex control mechanisms in which genes and mechanical forces provide control.

The final level of perfection might be the human form itself where specific features are thought to exist for specific reasons. One can say that the final function of a structure justifies its existence.

As for the skeletal adaptations within mankind, it was proposed that the relationship between physical forces and morphological modifications alter the design of an organism for its final function more than a century ago.

This “functional adaptation” of the individual bony setting was described to appear due to direct biological responses to mechanical stimuli like the long-term loading history of a skeleton.

Proof can be found in countless macroscopic saw-cut bony analysis over the century as they were performed by Julius Wolff, Wilhelm Roux, Peter Townsend or Giles Scuderi (to name just a few), who postulated that mechanical forces shape tissue bye the detailed observation that trabeculae match the principal stress lines. The tools to directly and individually test such ideas experimentally were not available at times, so interestingly, the development within the field of mechanobiology was linked to derived microscopic and medical imaging techniques almost one century later which lead to a recent renaissance in the field of mechanobiology.

This recently reacquired field of study developed itself into two different, but complemental directions.

One was the way of using the advanced techniques in “medical-imaging” to directly study the individual long-term loading history in relation to the linked anatomical representation of subchondral structures. Here, we showed within this thesis an adaptation of architectural parameters of bone in regards not only to the principal stress lines, but to the individual stress line distribution within the patella-femoral joint. Next to that, an alteration in the case of OA was also demonstrated, representing this system to be not only of a static, but highly dynamic nature.

By undertaking “medical-imaging” and “indentation-testing” investigations, we purposely decided to study the mechanobiology at a level of whole bones.
A level of analyzing bone so small, it reaches a cell biology level, is the second way that developed due so the newfound methods of microscopic methods. Here, the forces transmitted through the joint are divided down onto a cellular level and the genetic responses such as proliferation, differentiation and the metabolic activity as regulatory processes are assessed.
For bone, the above in detail described structural properties can be interpreted on a cellular level of investigation following the “Mechanobiology hypothesis” of Carter and Beauprê (1984, 2007). Hey proclaimed that the genetic disposition of bone, the biological component (r_b) is dominant during the juvenile growth period after been taken over by the mechanical component (r_m) after the growth cycle. The r_m following models the bone in a way to experience optimum strain levels via the strain energy density (SED). This SED is the summation of load intake moments that triggers a fluid flow within the widely spaced lacunae of bone which are interconnected. The resulting oscillatory fluid flow administers a cell response via streaming potentials, chemo-transport and wall shear stress. The latter is believed to stimulate a subsequent metabolic activity that leads to the delicate differentiation of each structural component until the systems experiences an optimum strain level due to the high degree of differentiation.
The resulting bony architecture stimulated by these processes is therefore in strong correlation to the load and strain distribution.

Despite this knowledge, it also has become clear, that most eukaryotic cells can generate intracellular force that act on the surrounding extracellular matrix and neighboring cells which seems critical for cell migration, differentiation and self-renewal. If due to cartilage degeneration the r_m is altered and OA arises, this self-generated intracellular force might be the key to trigger bone renewal.
So, after investigating the adaptation of bone on a level of whole bones, the future will undoubtedly be the investigation of the cellular level.

7 Abbreviations

General abbreviations

Ø	-	arithmetic mean
r^2	-	coefficient of determination
CT-OAM	-	computed tomography-osteoabsorptiometry
OA	-	osteoarthritis / osteoarthritic
OU	-	osteochondral unit
PFJ	-	patello-femoral joint
SBP	-	subchondral bone plate

Structural bone parameters

BV/TV	-	bone volume per total volume
DA	-	degree of anisotropy
SMI	-	structure model index
Tb.N	-	trabecular number
Tb.Sp.	-	trabecular spacing
Tb.Th.	-	trabecular thickness

Numerical abbreviations

2D	-	two-dimensional
3D	-	three-dimensional

8 References

1. Wolff J. Über die Architectur der Knochen und ihre Bedeutung für die Frage vom Knochenwachstum. Virchows Arch. 1877;50:389-450.
2. Wolff J. The law of bone remodelling. Berlin ; New York: Springer-Verlag; 1986.
3. Pauwels F. Eine neue Theorie über den Einfluß mechanischer Reize auf die Differenzierung der Stützgewebe. Zeitschrift für Anatomie und Entwicklungsgeschichte. 1960;121(6):478-515.
4. Tillmann B. [The stress of the human elbow joint. I. Functional morphology of the articular surfaces]. Zeitschrift fur Anatomie und Entwicklungsgeschichte. 1971;134(3):328-42.
5. Carter DR, Orr TE, Fyhrie DP. Relationships between loading history and femoral cancellous bone architecture. Journal of biomechanics. 1989;22(3):231-44.
6. WARD F. Outlines of human osteology. London 1838. WYmAn, J: On the can.
7. Wolff J. The law of bone remodelling: Springer Science & Business Media; 2012.
8. Pauwels F. Biomechanics of the locomotor apparatus: contribution on the functional anatomy of the locomotor apparatus. Berlin: Spfinger-Verlag. 1980.
9. Duncan H, Jundt J, Riddle JM, Pitchford W, Christopherson T. The tibial subchondral plate. A scanning electron microscopic study. J Bone Joint Surg Am. 1987 Oct;69(8):1212-20.
10. Outerbridge RE. The etiology of chondromalacia patellae. 1961. Clinical orthopaedics and related research. [Biography Classical Article Historical Article Portraits]. 2001 Aug(389):5-8.
11. Clark JM, Huber JD. The structure of the human subchondral plate. J Bone Joint Surg Br. 1990 Sep;72(5):866-73.
12. Madry H, van Dijk CN, Mueller-Gerbl M. The basic science of the subchondral bone. Knee Surg Sports Traumatol Arthrosc. 2009 Apr;18(4):419-33.
13. Müller-Gerbl M. The subchondral bone plate. Berlin ; New York: Springer; 1998.
14. Pauwels F. Gesammelte abhandlungen zur funktionellen anatomie des bewegungsapparates: Springer-Verlag; 2013.
15. Müller-Gerbl M, Schulte E, Putz R. The thickness of the calcified layer of articular cartilage: a function of the load supported? Journal of anatomy. 1987;154:103.
16. Shepherd D, Seedhom B. Thickness of human articular cartilage in joints of the lower limb. Annals of the rheumatic diseases. 1999;58(1):27-34.

17. Simkin PA, Graney DO, Fiechtner JJ. Roman arches, human joints, and disease. Arthritis & Rheumatism. 1980;23(11):1308-11.
18. Dewire P, Simkin PA. Subchondral plate thickness reflects tensile stress in the primate acetabulum. Journal of orthopaedic research. 1996;14(5):838-41.
19. Duncan H, Riddle J, Pitchford W. Osteoarthritis and the subchondral plate. Degenerative joints. 1985;2:181-97.
20. Milz S, Putz R. Quantitative morphology of the subchondral plate of the tibial plateau. Journal of anatomy. 1994;185(Pt 1):103.
21. Schunke M, Tillmann B, Schleicher A, Pointner H. Biomechanische und histochemische Untersuchungen am Tibiaplateau des Menschen. Verh Anat Ges. 1987;81:451-3.
22. Oberlander W. [The stress of the human hip joint. V. The distribution of bone density in the human acetabulum (author's transl)]. Z Anat Entwicklungsgesch. 1973 Aug 30;140(3):367-84.
23. Zumstein V, Kraljevic M, Huegli R, Muller-Gerbl M. Mineralisation patterns in the subchondral bone plate of the humeral head. Surg Radiol Anat. 2011 May 18.
24. Carter DR, Orr TE, Fyhrie DP. Relationships between loading history and femoral cancellous bone architecture. J Biomech. 1989;22(3):231-44.
25. Pauwels F. Gesammelte Abhandlungen zur funktionellen Anatomie des Bewegungsapparates. Berlin, New York,: Springer-Verlag; 1965.
26. Noble J, Alexander K. Studies of tibial subchondral bone density and its significance. J Bone Joint Surg Am. 1985;67(2):295-302.
27. Zumstein V, Kraljević M, Müller-Gerbl M. Glenohumeral relationships: subchondral mineralization patterns, thickness of cartilage, and radii of curvature. Journal of Orthopaedic Research. 2013;31(11):1704-7.
28. Aglietti P, Buzzi R, Insall J. Disorders of the patellofemoral joint. Surgery of the knee. 2001;1:913-1043.
29. Nowakowski AM, Deyhle H, Zander S, Leumann A, Müller-Gerbl M. Micro CT analysis of the subarticular bone structure in the area of the talar trochlea. Surgical and Radiologic Anatomy. 2013;35(4):283-93.
30. Muller-Gerbl M. The subchondral bone plate. Adv Anat Embryol Cell Biol. [Review]. 1998;141:III-XI, 1-134.
31. HUNGERFORD DS, BARRY M. Biomechanics of the patellofemoral joint. Clinical orthopaedics and related research. 1979;144:9-15.

32. Scuderi GR. The patella: Springer Science & Business Media; 1995.
33. Fox AJ, Wanivenhaus F, Rodeo SA. The basic science of the patella: structure, composition, and function. Journal of Knee Surgery. 2012;25(2):127.
34. HEHNE H-J. Biomechanics of the patellofemoral joint and its clinical relevance. Clinical orthopaedics and related research. 1990;258:73-85.
35. Hefzy M, Jackson W, Saddemi S, Hsieh Y-F. Effects of tibial rotations on patellar tracking and patello-femoral contact areas. Journal of biomedical engineering. 1992;14(4):329-43.
36. Fitzpatrick CK, Baldwin MA, Ali AA, Laz PJ, Rullkoetter PJ. Comparison of patellar bone strain in the natural and implanted knee during simulated deep flexion. Journal of Orthopaedic Research. 2011;29(2):232-9.
37. Borotikar B, Sheehan F. In vivo patellofemoral contact mechanics during active extension using a novel dynamic MRI-based methodology. Osteoarthritis and Cartilage. 2013;21(12):1886-94.
38. Eckstein F, Muller-Gerbl M, Putz R. Distribution of subchondral bone density and cartilage thickness in the human patella. Journal of anatomy. 1992 Jun;180 (Pt 3):425-33.
39. Ficat RP, Hungerford DS. Disorders of the patello-femoral joint: Williams & Wilkins Baltimore; 1977.
40. Raux P, Townsend PR, Miegel R, Rose RM, Radin EL. Trabecular architecture of the human patella. Journal of biomechanics. 1975 Jan;8(1):1-7.
41. Sun HB. Mechanical loading, cartilage degradation, and arthritis. Annals of the New York Academy of Sciences. 2010;1211(1):37-50.
42. Valderrabano V, Horisberger M, Russell I, Dougall H, Hintermann B. Etiology of ankle osteoarthritis. Clinical Orthopaedics and Related Research®. 2009;467(7):1800-6.
43. Radin EL, Parker HG, Pugh JW, Steinberg RS, Paul IL, Rose RM. Response of joints to impact loading—III: Relationship between trabecular microfractures and cartilage degeneration. Journal of biomechanics. 1973;6(1):51IN955-54IN1157.
44. Burr DB, Martin RB, Schaffler MB, Radin EL. Bone remodeling in response to in vivo fatigue microdamage. Journal of biomechanics. 1985;18(3):189-200.
45. Fazzalari N, Parkinson I. Fractal properties of subchondral cancellous bone in severe osteoarthritis of the hip. Journal of Bone and Mineral Research. 1997;12(4):632-40.

46. Kamibayashi L, Wyss U, Cooke T, Zee B. Trabecular microstructure in the medial condyle of the proximal tibia of patients with knee osteoarthritis. Bone. 1995;17(1):27-35.
47. Bobinac D, Spanjol J, Zoricic S, Maric I. Changes in articular cartilage and subchondral bone histomorphometry in osteoarthritic knee joints in humans. Bone. 2003;32(3):284-90.

9 Acknowledgements

"When life gives you lemons, make lemonade"

Elbert Hubbarb - 1915

Just because there is a quote heading does not mean that something intellectual will follow, but in this case it is very well put here.
When I was firstly confronted with the idea of a PhD-program, I did not at all oversee what would be coming, or better: how much would be coming. Right from the start, I found lemons all over the way, and even if it sounds simple to squeeze them and add sugar, it is not always possible on your own.

I am thankful to everyone who contributed in one way or the other to this PhD thesis and supported me. I would particularly like to mention and thank the following:

Firstly, a big “Thank you!” goes to my supervisor and mentor, *Magdalena Müller-Gerbl*. In her endless reinforcement and motivation as well as input and help, she opened the right doors at the right time and made this project possible. I deeply appreciate everything you have done for me and especially are thankful for your ongoing support during the hard times.
Thank you for never letting me down!
Secondly, “Thank you!” to *Mireille Toranelli*. I know it has not always been easy to try to teach me Analyze, and so much more.
Merci beaucoup! For your patients with my MMA abilities and for always listening to me.
More than half of my data has been acquired at the Biomaterial Science Center, where I was always welcome and found help. So I thank *Bert Müller* for his time and effort in correcting my manuscripts and guiding my PhD into the right direction.
The lectures at ETH have been a pleasure, even though you sometimes reached my limits. Thank you!
Furthermore, I would like to kindly thank *Georg Schulz* for helping me with every technical nanotom-problem I faced and caused, as well as *Hans Deyhle* for his support when I failed in my programming skills.
In addition, thank you *Simone* for coordinating and *Anna* for opening doors, even on the weekends.

The mechanical strength tests were made possible by *Beat Göpfert* and *Dieter Wirz* from the “Department of mechanical properties of natural & engineered tissues & related materials, mechanics of implant/tissue interfaces”. Thank you for all the know-how and the help with broken needles and moving ball joints.

Furthermore, “Thank you!” to *Reinhard Putz*, my external expert. I enjoyed our stimulating talks and appreciate the time you spend over my documents.

And… there are so many more:

Piotr Maly	for always being understanding when I did not understand, the coffee breaks and for doing my work when time was sparse
Peter Zimmermann	for always having an open ear for my problems and undoubting support whatever idea I came up with
Roger Kurz	for always thinking about me with samples and patiently explaining how things are done
Amit Patel	for his incredible knowledge whenever I had questions and for the time he spend over my documents - Thanks mate!
Sandra Blache	for usually keeping me from my work, but for always being there for me…

Thank you! Danke vielmals! Merci beaucoup!

Last but not least:

“Thank You!” to my *parents,* for their love and encouragement!

10 Affirmation about the usage of material

Schriftliche Erklärung

Ich erkläre, dass ich die Dissertation

"Multi-parameter topographical analysis of the subchondral bone in healthy and osteoarthritic human patellae"

nur mit der darin angegebenen Hilfe verfasst und bei keiner anderen Universität und keiner anderen Fakultät der Universität Basel eingereicht habe.

Ich bin mir bewusst, dass eine unwahre Erklärung rechtliche Folgen haben kann.

Basel, 04.06.2018 Sebastian Höchel

11 Appendix

11.1 Additional publications

Wiewiorski M, **Hoechel S**, et al. “Computed Tomographic Evaluation of Joint Geometry in Patients With End-Stage Ankle Osteoarthritis.“ Foot Ankle Int. 2016

Hauser NH, **Hoechel S**, et al. “Functional and Structural Details about the Fabella: What the Important Stabilizer Looks Like in the Central European Population.“ Biomed Res Int. 2015

Wiewiorski M, Hiebinger A, **Hoechel S**, et al. “Transcutaneous pleural biopsy with a retrograde forceps: a novel approach.” Surg Endosc. 2015

Leumann A, Valderrabano V, **Hoechel S**, et al. “Mineral density and penetration strength of the subchondral bone plate of the talar dome: high correlation and specific distribution patterns.” J Foot Ankle Surg. 2015

Zumstein V, Kraljević M, **Hoechel S**, et al. “The glenohumeral joint - a mismatching system? A morphological analysis of the cartilaginous and osseous curvature of the humeral head and the glenoid cavity.” J Orthop Surg Res. 2014

Zumstein V, Kraljević M, Conzen A, **Hoechel S**, et al. “Thickness distribution of the glenohumeral joint cartilage: a quantitative study using computed tomography.” Surg Radiol Anat. 2014

Mueller F, **Hoechel S**, et al. “The subtalar and talonavicular joints: a way to access the long-term load intake using conventional CT-data.“ Surg Radiol Anat. 2014

Hoechel S, Schulz G, et al. “Dreidimensionale Analyse knöcherner Gewebe post mortem.“ Swiss Medical Forum, 2013.

Hoechel S, Alder M, et al. “The human hip joint and its long term load intake - how X-ray density distribution mirrors bone strength.“ Hip Int., 2013.

Wiewiorski M, **Hoechel S**, et al. “Computer tomographic evaluation of talar edge configuration for osteochondral graft transplantation.“ Clin Anat. 2012

11.2 Curriculum vitae

Dr. med. Sebastian Höchel

Date of Birth: September 30th, 1981
Place of Birth: Teterow, Germany

Mail Address:
Zilstrasse 20
CH-9016 Sankt Gallen
sebastian.hoechel@unibas.ch
Mobile: +4178 682 7117

Language: German (mother tongue), English (fluent), Russian (basic understanding)

Current Positions

Since 05/2018	Clinical Residency in General Surgery, Department of Surgery, Spitalverbund Appenzell Ausserrhoden, Spital Herisau, Switzerland
02/2017 – 01/2018	Clinical Residency in Orthopedic Surgery, Department of Orthopedic Surgery and Traumatology, Universitätsspital Basel, Basel, Switzerland
02/2016 – 01/2017	Clinical Residency in General Surgery, Department of Surgery, Hirslanden Klinik Stephanshorn, Sankt Gallen, Switzerland
02/2015 – 01/2016	Universitätsdozent, Institute of Anatomy, Department of Biomedicine, University of Basel, Switzerland
01/2011 – 01/2015	PhD Candidate, Institute of Anatomy, Department of Biomedicine, University of Basel, Switzerland
07/2010 – 12/2010	Clinical Residency in General Surgery, Department of Surgery, Spital Wil, Sankt Gallen, Switzerland
01/2010 – 06/2010	Research Assistant (Doctoral Fellow), “Osteoarthritis Research Group”, University of Basel, Switzerland

04/2009 – 07/2009	Clinical Internship, Intensive Care Unit, University Hospital Rostock, Germany
12/2008 – 03/2009	Clinical Internship, Department of Internal Medicine, Spital Wil, Sankt Gallen, Switzerland
08/2008 – 11/2008	Clinical Internship, Department of Surgery, Spital Wil, Sankt Gallen, Switzerland
07/2001 – 09/2002	Support Worker, “St. Christopher’s School” for children with severe learning difficulties and physical disabilities, Bristol, Great Britain

Education

10/2002 – 07/2009	Medical School University of Rostock, Germany
06/2001	High School Graduation, Gymnasium Grosse Stadtschule Rostock, Germany

Diploma

2012	Medical Doctor Thesis, University of Basel “Computer Tomographic Evaluation of Talar Edge Configuration for Osteochondral Graft Transplantation”
2009	Final Boards in Medicine, Medical License

Basel, June 4th 2018

Sebastian Höchel

11.3 Rights and Permissions

Figure preamble: “Springer eBook “100 Jahre Transformationsgesetz der Knochen“ von Julius Wolff, Licensed content date: Jan 1, 1993, Licensed content author: D. Wessinghage, Original figure number: figure 1, License Number: 3751460318885; with kind permission from Springer Science and Business Media”

Figure 1, 2: “Springer eBook “The Internal Architecture of Normal Bone and Its Mathematical Significance“, Licensed content date: Jan 1, 1986, Licensed content author: Julius Wolff, Original figure numbers: figures 2, 7, 9, License Number: 3751441330161; with kind permission from Springer Science and Business Media”

Figure 3: With kind regards to the:

Musculoskeletal Research Group
Department of Biomedicine
University of Basel
Pestalozzistrasse 20
CH - 4056 Basel

Figure preparation: Figures 4, 5, and 6 were created with help of:

Advanced visualization and analysis software
AnalyzeDirect, Inc.
7380 W 161st Street
Overland Park, KS, 66085
United States

Volume Graphics GmbH
Speyerer Strasse 4 – 6
69115 Heidelberg
Germany